

The official publication of the
Hong Kong Academy of Medicine and
the Hong Kong Medical Association

HONG KONG

MEDICAL JOURNAL

香港醫學雜誌

21(3)

HONG KONG MEDICAL JOURNAL

香港醫學雜誌

Volume 21 Number 3 June 2015

Research Fund for the Control of Infectious Diseases

Research Dissemination Reports

控制傳染病研究基金

研究成果報告

Respiratory Infectious Diseases
呼吸道傳染病

Gastrointestinal Diseases
腸胃病

Viral Hepatitis
病毒性肝炎

Miscellaneous Infection
其他感染

ISSN 1024-2708



香港醫學專科學院出版社
HONG KONG ACADEMY OF MEDICINE PRESS

Supplement 4

MEDICAL JOURNAL

香港醫學雜誌

EDITOR-IN-CHIEF

Ignatius TS Yu 余德新

SENIOR EDITORS

PT Cheung 張璧濤
 Albert KK Chui 徐家強
 Michael G Irwin
 Martin CS Wong 黃至生
 TW Wong 黃大偉

EDITORS

Gavin J Chan 陳慶釗
 KL Chan 陳廣亮
 KS Chan 陳健生
 Henry LY Chan 陳力元
 David VK Chao 周偉強
 W Cheuk 卓華
 TW Chiu 趙多和
 Paul CL Choi 蔡祥龍
 Stanley ST Choi 蔡兆堂
 LW Chu 朱亮榮
 Ellis KL Hon 韓錦倫
 KW Huang 黃凱文
 WK Hung 熊維嘉
 Bonnie CH Kwan 關清霞
 Alvin KH Kwok 郭坤豪
 Paul BS Lai 賴寶山
 Eric CH Lai 賴俊雄
 CY Lam 林楚賢
 Stephen TS Lam 林德深
 Patrick CP Lau 劉志斌
 Arthur CW Lau 劉俊穎
 Keith KH Lau 劉廣洪
 PY Lau 婁培友
 Nelson LS Lee 李禮舜
 Danny WH Lee 李偉雄
 KY Leung 梁國賢
 Danny TN Leung 梁子昂
 Thomas WH Leung 梁慧康
 WK Leung 梁惠強
 Kenneth KW Li 李啟煌
 David TL Liu 劉大立
 Janice YC Lo 羅懿之
 Herbert HF Loong 龍浩鋒
 James KH Luk 陸嘉熙
 Andrea OY Luk 陸安欣
 Ada TW Ma 馬天慧
 Arthur DP Mak 麥敦平
 Henry KF Mak 麥嘉豐
 Anthony CF Ng 吳志輝
 Jacobus KF Ng 吳國夫
 Hextan YS Ngan 顏婉嫦
 Martin W Pak 白威
 Edward CS So 蘇超駒
 William YM Tang 鄧旭明
 Kenneth KY Wong 黃格元
 Patrick CY Woo 胡釗逸
 Bryan PY Yan 甄秉言
 TK Yau 游子覺
 Kelvin KH Yiu 姚啟恒

ADVISORS ON BIOSTATISTICS

William B Goggins
 Eddy KF Lam 林國輝

ADVISOR ON CLINICAL EPIDEMIOLOGY

Shelly LA Tse 謝立亞

Research Fund for the Control of Infectious Diseases**Research Dissemination Reports****Editorial**

3

RESPIRATORY INFECTIOUS DISEASES**Molecular tests for rapid detection of rifampicin and isoniazid resistance in *Mycobacterium tuberculosis***

4

*PL Ho, WC Yam, CC Leung, WW Yew, TYW Mok, KS Chan, CM Tam***Direct identification and quantification of host and viral miRNAs after influenza infection using the next generation ultra-high throughput DNA sequencer**

8

*MY Lee, S Lok, CY Cheung***H5N1 virus resistant to antiviral drug**

12

*HL Chen, Y Guan***Live recombinant *Salmonella* oral vaccine against avian influenza viruses**

14

*JD Huang, BJ Zheng, KY Yuen***GASTROINTESTINAL DISEASES****The role of cathelicidin in control of *Helicobacter pylori* colonisation in the stomach**

17

*CH Cho, J Yu, L Zhang, WKK Wu***Institutional risk factors for outbreaks of acute gastroenteritis in homes for the elderly: a retrospective cohort analysis**

20

*LW Tian, WY Wong, SC Ho, S Ng, WM Chan***VIRAL HEPATITIS****Liver cirrhosis-specific glycoforms of serum proteins in chronic hepatitis B infection: identification by lectin affinity chromatography and quantitative proteomic profiling**

22

*TCW Poon, HLY Chan, HWC Leung, A Lo, RHY Lau, AY Hui, JY Sung***Role of hepatitis B virus X protein in liver cancer**

27

*IOL Ng, KMF Sze, GKY Chui***Viral mutant discovery in hepatitis B virus quasi-species in patients undergoing long-term lamivudine treatment**

31

*CM Ding, JY Sung, HLY Chan, J Luan***Identification of hepatitis B virus DNA reverse transcriptase variants associated with partial response to entecavir**

35

DKH Wong, J Fung, CL Lai, MF Yuen

**INTERNATIONAL EDITORIAL
ADVISORY BOARD**

Sabaratnam Arulkumaran
United Kingdom

Robert Atkins
Australia

Peter Cameron
Australia

David Christiani
United States

James Dickinson
Canada

Willard Fee, Jr
United States

Robert Hoffman
United States

Sean Hughes
United Kingdom

Arthur Kleinman
United States

Xiaoping Luo
China

Jonathan Samet
United States

Max Wintermark
United States

Homer Yang
Canada

MISCELLANEOUS INFECTION

Modulation of cytokine responses by adrenomedullin and adrenomedullin binding protein-1 in macrophages: a novel pathway in sepsis 39
LYF Wong, BMY Cheung

Association of human adenovirus-36 with diabetes, adiposity, and dyslipidaemia in Hong Kong Chinese 45
MMY Waye, JCN Chan, PCY Tong, R Ma, PKS Chan

Author index & Disclaimer 48

MANAGING EDITOR

Yvonne Kwok 郭佩賢

DEPUTY MANAGING EDITOR

Betty Lau 劉薇薇

ASSISTANT MANAGING EDITOR

Warren Chan 陳俊華

Editorial

Dissemination reports are concise informative reports of health-related research supported by funds administered by the Food and Health Bureau, for example the *Research Fund for the Control of Infectious Diseases* (which was consolidated into the *Health and Medical Research Fund* in December 2011). In this edition, 12 dissemination reports of projects related to respiratory infectious diseases, gastrointestinal diseases, viral hepatitis, and miscellaneous infection are presented. In particular, three projects are highlighted due to their potentially significant findings, impact on healthcare delivery and practice, and/or contribution to health policy formulation in Hong Kong.

Multidrug-resistant tuberculosis often entails prolonged treatment and the use of more toxic drugs. It is also associated with higher rates of treatment failure and death. As the mechanisms for rifampicin (RIF) and isoniazid (INH) resistance in many isolates of *Mycobacterium tuberculosis* are predictable, molecular methods are used for direct detection of RIF and INH resistance. Ho et al¹ evaluated genotypic tests to detect RIF and INH resistance in *M. tuberculosis* in clinical specimens. The rapid tests improved patient management by enabling earlier admission, more timely use of World Health Organization category IV antituberculosis regimens, and discontinuation of ineffective drugs.

Helicobacter pylori infection is associated with gastritis, gastric and duodenal ulcers, and gastric cancer. The effect of host factors on colonisation with *H. pylori* remains poorly understood. Cho et al² studied the effect of cathelicidin, a host defence

peptide, on *H. pylori* colonisation in an animal model. Deficiency of cathelicidin enhanced *H. pylori* infection and inflammation in the gastric mucosa. Oral delivery of cathelicidin-secreting bacteria reduced *H. pylori* infection and gastric inflammation. The authors obtained a patent in relation to this study.

Entecavir is an oral reverse transcriptase inhibitor used in the treatment of hepatitis B virus (HBV) infection. Wong et al³ found that 21% of HBV-infected patients had detectable HBV DNA after 1 year of entecavir therapy. Twenty reverse transcriptase variants were found exclusively in entecavir partial responders, and four variants had significantly different distribution among optimal and partial responders. Further in-depth studies are required to confirm the significance of the results.

A research impact evaluation was conducted 2 years after the project end date for all of the studies reported in this supplement. Impact was reported through knowledge generation, capacity building, and influence on health policy and health care practices through changes in behaviour of health care professionals and/or other decision makers.

We hope you will enjoy this selection of research dissemination reports. Electronic copies of these dissemination reports and the corresponding full reports can be downloaded individually from the Research Fund Secretariat website (<http://www.fhb.gov.hk/grants>). Researchers interested in the funds administered by the Food and Health Bureau also may visit the website for detailed information about application procedures.

Supplement co-editors



Dr Ivy Cheung
Chief Secretariat Executive
(Research Office)
Food and Health Bureau



Dr Richard A. Collins
Scientific Review Director
(Research Office)
Food and Health Bureau

References

1. Ho PL, Yam WC, Leung CC, et al. Molecular tests for rapid detection of rifampicin and isoniazid resistance in *Mycobacterium tuberculosis*. *Hong Kong Med J* 2015;21(Suppl 4):4-7.
2. Cho CH, Yu J, Zhang L, Wu WK. The role of cathelicidin in

control of *Helicobacter pylori* colonisation in the stomach. *Hong Kong Med J* 2015;21(Suppl 4):17-9.

3. Wong DK, Fung J, Lai CL, Yuen MF. Identification of hepatitis B virus DNA reverse transcriptase variants associated with partial response to entecavir. *Hong Kong Med J* 2015;21(Suppl 4):35-8.

Molecular tests for rapid detection of rifampicin and isoniazid resistance in *Mycobacterium tuberculosis*

PL Ho *, WC Yam, CC Leung, WW Yew, TYW Mok, KS Chan, CM Tam

KEY MESSAGES

1. In patients suspected to have tuberculosis, a valid molecular test result was obtained in 94.3% and 88.3% of patients for the *rpoB* and *katG* loci, respectively, for prediction of drug susceptibility.
2. Molecular testing based on *katG* and *rpoB* enabled rapid detection of *Mycobacterium tuberculosis* resistance in 46.8% and 87.5% of patients infected with isoniazid- and rifampicin-resistant strains, respectively. The same number of patients infected with resistant strains with mutations in *katG* and *rpoB* were detected using the MTBDRplus line probe assay. The combined use of *katG* and *inhA* regulatory region in the MTBDRplus line probe assay increased the proportion of patients identified with INH-resistant MTB strains to 72.3%.

3. The rapid tests improved patient management by enabling earlier admission, more timely use of World Health Organization category IV anti-tuberculosis regimens and discontinuation of ineffective drugs.

Hong Kong Med J 2015;21(Suppl 4):S4-7

RFCID project number: 04050032

¹ PL Ho *, ¹ WC Yam, ² CC Leung, ³ WW Yew, ⁴ TYW Mok, ⁵ KS Chan, ² CM Tam

¹ Department of Microbiology, University of Hong Kong

² TB and Chest Service, Department of Health

³ TB and Chest Unit, Grantham Hospital

⁴ Respiratory Medical Department, Kowloon Hospital

⁵ Haven of Hope Hospital

* Principal applicant and corresponding author: plho@hku.hk

Introduction

Multidrug-resistant tuberculosis (MDR-TB) often entails prolonged treatment and the use of more toxic drugs. It is also associated with higher rates of treatment failure and death. The World Health Organization category I regimens for the management of MDR-TB are inadequate. In British Medical Research Council studies, only three of the 11 patients with MDR-TB were cured when prescribed standard treatment. Early recognition of resistance and administration of two or more drugs have improved patient outcome. It is important to reduce the turn-around time for reporting anti-tuberculosis drug susceptibility. Cultures are the gold standard for susceptibility testing, but they are limited by the pre-requisite for a pure growth from clinical specimens. As the mechanisms for rifampicin (RIF) and isoniazid (INH) resistance in many isolates of *Mycobacterium tuberculosis* (MTB) are predictable, molecular methods are used for direct detection of RIF and INH resistance. This study evaluated genotypic tests to detect RIF and INH resistance in MTB in clinical specimens. The potential impact of implementing molecular tests to detect RIF and INH resistance in MTB was also assessed.

Methods

This study was conducted from April 2006 to June

2009. Patients were prospectively identified from 15 participating centres at the tuberculosis and chest unit of the Department of Health, the Grantham Hospital, the Kowloon Hospital, and the Haven of Hope Hospital. Adult patients suspected to have active tuberculosis and were at risk of infection with INH- and/or RIF-resistant strains were enrolled. Clinical specimens (sputum or other appropriate samples) were tested by polymerase chain reaction (PCR) assays specific for IS6110, *rpoB*, and *katG*. The amplicons were sequenced to detect resistance mutations. PCR and sequencing were conducted on a weekly basis. Specimens with resistant strains were also tested by the MTBDRplus and the INNO-LiPA Rif.TB line probe assays. Acid-fast bacillus smear and mycobacterial culture were performed by conventional methods.

Results

Patient demographics and sensitivity of the PCR assays

A total of 820 specimens (>90% respiratory) were obtained from 720 patients. In 596 (82.7%) patients, the culture was positive for MTB. Using the culture and susceptibility testing result as reference, the overall sensitivity of the IS6110, *rpoB*, and *katG* PCR assays was 98.9%, 95.9%, and 88.7%, respectively (Table 1). 94.3% (562/596) and 88.3% (526/596) of

patients had valid molecular test results for the *rpoB* and *katG* loci, respectively.

Susceptibility testing revealed that 50 patients were infected with strains resistant to INH and/or RIF, including MDR-TB (INH-R/RIF-R) [n=13], INH-R/RIF-S (n=34), and INH-S/RIF-R (n=3). The remaining 542 MTB isolates were susceptible to both INH and RIF.

Correlation between susceptibility testing and *rpoB* mutations

Among 562 valid molecular *rpoB* test results, the concordance rate with susceptibility testing was 99.5% (559/562). Mutations were found in codons 531, 533, 526, and 516 within the *rpoB* hotspot region. The discordant results involved three patients with RIF-susceptible isolates and one of two mutations (L533P and H526N). All *rpoB* mutations, including the three discordant results, were confirmed by testing the purified isolates. Fourteen (87.5%) of 16 patients infected with RIF-resistant strains were detected by the PCR-sequencing method. The detection rate for *rpoB* mutation was the same using the GenoType MTBDRplus test.

Among 527 valid molecular *katG* test results, the concordance rate with susceptibility testing was 97.2% (512/527). Our *katG* PCR assay could

rapidly detect resistance in only 22 (46.8%) of the 47 patients infected with INH-resistant strains. The same number (ie 22) of *katG* mutations was detected using the GenoType MTBDRplus test, which also detected an additional 12 patients with mutations in the promoter region of *inhA*. Therefore, INH resistance was correctly predicted by the GenoType MTBDRplus test in 34 (72.3%) of the 47 patients.

Impact on patient management

Overall, 50 patients had a positive culture for MTB isolates resistant to INH and/or RIF. Susceptibility testing revealed that 34 isolates were resistant to INH alone, three to RIF alone, and 13 to both INH and RIF (ie MDR-TB). 92% and 80% of the 50 patients had a valid result for *rpoB* and *katG* mutations, respectively. The genotypic results according to PCR-sequencing correctly predicted *rpoB* resistance mutations in 15 specimens and *katG* resistance mutations in 22 specimens. These mutations involved 32 patients and the correlation with the susceptibility result is summarised in Table 2. The mean±standard deviation (SD) turnaround time was 10.2±5 days for *rpoB* and 9.5±4.8 days for *katG*. This was significantly shorter than the interval between first sputum specimen and susceptibility test reporting (15.4±5.4 weeks). This enables earlier

TABLE 1. Comparative sensitivity of three polymerase chain reaction (PCR) assays for detection of *Mycobacterium tuberculosis* (MTB)

Parameter	No. (%) of patients								
	Positive results			<i>rpoB</i> mutation			<i>katG</i> Thr315		
	IS6110 PCR	<i>rpoB</i> PCR	<i>katG</i> PCR	Present	Absent	Indeterminate	Present	Absent	Indeterminate
MTB culture-positive (n=596)	590 (98.9)	572 (95.9)	529 (88.8)	17	545	10	21	505	3
Smear-positive (n=538)	538 (100)	532 (98.8)	503 (93.5)	16	512	4	19	482	2
Smear-negative (n=58)	52 (89.6)	40 (68.9)	26 (44.8)	1	33	6	2	23	1
MTB culture-negative (n=124)*	66	54	41	0	53	1	0	41	0
Total	656 (91.1)	626 (86.9)	570 (79.2)	17	598	11	21	546	3

* In 13 patients, the culture was positive for non-tuberculous mycobacteria

TABLE 2. Correlation between polymerase chain reaction–sequencing for *rpoB* and *katG* mutations and susceptibility testing in 32 patients infected with *Mycobacterium tuberculosis* resistant to isoniazid and/or rifampicin

Genotypic result obtained by testing of respiratory specimens		No. of phenotypic result obtained by susceptibility testing		
<i>rpoB</i>	<i>katG</i>	Isoniazid-resistant (n=17)	Rifampicin-resistant (n=3)	Multidrug-resistant (n=12)
Mutated	Mutated	-	-	4
Mutated	Wild type	-	3	4
Indeterminate	Mutated	-	-	1
Mutated	Indeterminate	-	-	3
Wild type	Mutated	17	-	-

TABLE 3. Potential impact of molecular testing for *Mycobacterium tuberculosis* resistance mutations on patient management for seven representative cases

Case No.	Sex/age (years)	History of tuberculosis	Risk factors for resistant tuberculosis	Genotypic test on sputum				Anti-tuberculosis treatment		Remarks
				IS6110	rpoB	katG	gyrA	At testing	After testing	
26	M/30	Yes	Multiple treatment in China	Positive	S531L	S315T	Mutated	None	Category IV	Multidrug-resistant tuberculosis (MDR-TB); individualised category IV treatment started 1 week after patient presentation
11	M/66	No	Persistent smear positivity	Positive	WT	S315T	-	Category I	Stop isoniazid	Test result contributed to individualised regimen decision
14	F/48	Yes	Previous treatment in China	Positive	D516A	S315N	-	Category II	Category IV	MDR-TB; test result contributed to individualised regimen decision
28	F/50	No	-	Positive	S531L	WT	-	Category I	Category IV	Polydrug resistant tuberculosis; test result contributed to individualised regimen decision
29	M/30	No	Extensive disease	Positive	S531L	Indeterminate	-	Category I	Category IV	MDR-TB; patient admitted for individualised treatment because of test result
45	F/37	Yes	Failed category I regimen	Positive	S531L	WT	Mutated	Category IV	Category IV	Extensively drug-resistant tuberculosis; test result contributed to individualised regimen decision
50	M/70	Yes	Failed category I regimen	Positive	D516V	Indeterminate	-	Category I	Category IV	MDR-TB; culture and sensitivity testing was delayed because of mixed growth of <i>M tuberculosis</i> and <i>M gordonae</i> ; test result contributed to individualised regimen decision

patient isolation, admission for treatment, and discontinuation of inactive drugs (Table 3).

Discussion

In Hong Kong, diagnostic PCR is useful to detect MTB in clinical specimens.¹ This study extended this by inclusion of two PCR assays specific for rpoB and katG genes to determine whether there were mutations associated with resistance to RIF and INH. Using culture and drug susceptibility results as reference, 94.3% and 88.3% of patients had valid molecular test results for the rpoB and katG loci, respectively. The result for both rpoB and katG was highly concordant with the conventional susceptibility result.²

As RIF and INH resistance could occur as a result of mutations in multiple gene loci, the specificity of molecular assays (as compared with susceptibility testing) would not be 100%. For RIF, a high degree of concordance between mutations in the rpoB hotspot region (codon 507-533) and phenotypic resistance was found. A rapid diagnosis was made for 87.5% of patients infected with RIF-resistant strains, as more than 96% of RIF-resistant strains have mutations in this region.³ In another three patients infected with phenotypic RIF-susceptible strains, the rapid test identified rpoB mutations (L533P or H526N), which were uncommon. The molecular assay results were reliable because identical mutations were confirmed by testing the isolates. These infrequent

rpoB mutations may cause weak resistance to RIF and have the potential to cause highly discordant RIF susceptibility results, even when tested under proficiency evaluation settings by the Supra-National Tuberculosis Reference Laboratories.⁴ The MTBDRplus insert also indicated that the L533P mutation may be RIF-susceptible in susceptibility testing. Nonetheless, both L522P and H526N have been reported to cause high-level RIF resistance and to occur in MDR-TB strains.⁵ Further studies to assess the clinical significance of these low-level resistant isolates are necessary.

Unlike RIF resistance, the katG PCR assay could provide rapid diagnosis in only 22 (46.8%) of the 47 patients infected with INH-resistant strains. The same number of katG mutations was detected by the MTBDRplus assay. The inhA promoter region was included in the MTBDRplus assay as an additional target. This enabled detection of an additional 12 patients with INH-resistant infection. Thus, the MTBDRplus assay could rapidly detect INH resistance in 34 (72.3%) of the 47 patients. 38 of the 47 INH-resistant isolates were found to have mutations in the katG gene and/or the inhA regulatory region. Thus, even if the PCR assay was 100% sensitive in detecting mutations in katG and the promoter of inhA in clinical specimens, direct testing would at best identify 80.9% (38/47) of INH-resistant infections. To improve the sensitivity further, it is necessary to include other gene target in molecular assays. A tuberculosis drug resistance

database has been established.⁵ The INH-resistant strains with wild type *katG* and promoter region in *inhA* may have mutations in the *katG* outside the fragment that was sequenced, within the *inhA*, intergenic region of *oxyR-ahpC* or other genes.

Conclusions

The molecular test result is valid in most patients with suspected and confirmed tuberculosis. The test result for *rpoB* and *katG* is reliable and highly concordant with results using culture isolates. Molecular testing enables better management of patients infected with drug-resistant tuberculosis.

Acknowledgements

This study was supported by the Research Fund for the Control of Infectious Diseases, Food and Health Bureau, Hong Kong SAR Government (#04050032). We thank the doctors, nurses, and clerical and laboratory staff at the participating

centres for assistance with patient recruitment and data collection. We are grateful to Frankie Chow for excellent technical support, France Wong and Goretti Tse for dedicated secretarial assistance.

References

1. Cheng VC, Yam WC, Hung IF, et al. Clinical evaluation of the polymerase chain reaction for the rapid diagnosis of tuberculosis. *J Clin Pathol* 2004;57:281-5.
2. Lau RW, Ho PL, Kao RY, et al. Rapid diagnosis of multidrug-resistant smear-positive pulmonary tuberculosis. *Int J Antimicrob Agents* 2010;35:202-3.
3. Yam WC, Tam CM, Leung CC, et al. Direct detection of rifampin-resistant mycobacterium tuberculosis in respiratory specimens by PCR-DNA sequencing. *J Clin Microbiol* 2004;42:4438-43.
4. Van Deun A, Barrera L, Bastian I, et al. Mycobacterium tuberculosis strains with highly discordant rifampin susceptibility test results. *J Clin Microbiol* 2009;47:3501-6.
5. Sandgren A, Strong M, Muthukrishnan P, Weiner BK, Church GM, Murray MB. Tuberculosis drug resistance mutation database. *PLoS Med* 2009;6:e2.

Direct identification and quantification of host and viral miRNAs after influenza infection using the next generation ultra-high throughput DNA sequencer

MY Lee *, S Lok, CY Cheung

KEY MESSAGES

1. The host and viral whole transcriptomes (including miRNA and mRNA of pathogenic H5N1 and seasonal H1N1 influenza-virus-infected human macrophages) were quantified and compared.
2. A total of 43 new human miRNA candidates were discovered.
3. No miRNA was encoded by influenza viruses.
4. In response to H5N1 infection, the RIG-I-like receptor signalling pathway was the most

significant pathway regulated by known human miRNAs.

Hong Kong Med J 2015;21(Suppl 4):S8-11

RFCID project number: 08070532

¹ MY Lee *, ² S Lok, ¹ CY Cheung

¹ Centre of Influenza Research, Li Ka Shing Faculty of Medicine, The University of Hong Kong

² Li Ka Shing Institute of Health Sciences, The Chinese University of Hong Kong

* Principal applicant and corresponding author: suki@hku.hk

Introduction

The subtype of avian influenza H5N1 virus is epizootic and panzootic, and can transmit zoonotically to humans. The fatality rate of H5N1 disease remains high at about 60%, but this rate may be over-estimated, as H5N1 viruses cause both severe and subclinical infection in humans, and these mild non-hospitalised H5N1 cases are not counted by the World Health Organization as confirmed cases.¹

Cytokine dysregulation is one of the key contributory factors to H5N1 pathogenesis.² The precise mechanisms by which the H5N1 virus elicits the differential host responses remain poorly understood.

MicroRNAs (miRNAs) are 21-23 nt RNA molecules that can modulate gene expression and play an essential role in the regulation of many diverse biological processes, including viral infection. Macrophages are key host immune cells that respond to viral infection and are a major source of many cytokines. The present study used the new generation ultra-high throughput Solexa sequencer to determine host- and viral-derived miRNAs (if any) induced by the highly pathogenic H5N1 and low virulent H1N1 viruses in human macrophages at early time points. Together with the mRNA expression profile, the possible regulating pathways/mechanisms were revealed by identifying miRNAs that may lead to influenza pathogenesis.

Methods

This study was conducted from May 2009 to October 2011.

Virus infection of macrophages

Human macrophages were infected with H1N1 (A/HK/54/98) and H5N1 (A/Viet/3212/04) at a multiplicity of infection (MOI) of two. Cells and viruses were prepared as described previously.¹ After 30 minutes for virus adsorption, the inoculum was removed; cells were washed and incubated in macrophage serum-free medium (Invitrogen, CA, USA) supplemented with 0.6 mg/L penicillin and 60 mg/L streptomycin.

Total RNA isolation

Total RNA was extracted from cells 1, 3, and 6 hours post-infection using a *mirVana* miRNA Isolation Kit (Ambion, TX, USA) according to the manufacturer's instructions. The Agilent 2100 Bioanalyzer (Agilent Technologies, CA, USA) was used to assess RNA quality. All total RNA samples had a RNA Integrity Number (RIN) >9.0.

Ribosomal RNA depletion

Large 18S and 28S rRNAs were removed from 1 µg total RNA with the RiboMinus Transcriptome Isolation kit (Human/Mouse) (Invitrogen, CA, USA) according to the manufacturer's instructions. The rRNA-depleted RNA was precipitated with Pellet Paint (Novagen, WI, USA), quality checked on the Agilent 2100 Bioanalyzer (Agilent Technologies).

Illumina mRNA library preparation

The rRNA-depleted RNA from 1 µg of total RNA was fragmented by incubation for 5 minutes at 94°C

in 5 × Array Fragmentation Buffer (Ambion, TX, USA). The reaction was stopped by chilling the tube on ice and precipitated with Pellet Paint. Double strand cDNA was synthesised with the SuperScript Double Stranded cDNA synthesis kit (Invitrogen, CA, USA) using random hexamers according to the manufacturer's instructions. The reaction was cleaned up on a QiaQuick PCR column (Qiagen, CA, USA). Double-stranded cDNA fragments were repaired with DNA Terminator End Repair Kit End (Lucigen, WI, USA) by incubation for 30 minutes at 30°C and then cleanup on a QiaQuick PCR column. The Klenow 3' to 5' exo- (NEB, MA, USA) was used to add a single 'A' base to the 3' end of blunt phosphorylated DNA fragments by incubation for 30 minutes at 30°C. After clean-up on a QiaQuick PCR column, Illumina PE Adapter was ligated to the end of DNA fragments with the Quick Ligation Kit (NEB, MA, USA) by incubation for 15 minutes at room temperature. The reaction was cleaned up on a QiaQuick PCR column. 180-200 bp fragments were excised from a 2% low range agarose gel. Fragments were enriched by 10 cycles using AccuPrime Pfx DNA Polymerase (Invitrogen, CA, USA). The PCR product was run on Novex 8% TBE polyacrylamide gel and stained with SYBR Gold. The gel slice was cut off and cleaned up by QiaQuick Gel Extraction Kit. The concentration of gel purified DNA fragments was measured using a ND-1000 UV/Vis spectrophotometer (NanoDrop Technologies, DE, USA).

Illumina small RNA library preparation

A small RNA library was prepared from rRNA-depleted RNA from 1 µg of total RNA according to the Illumina manufacturer's instructions. The 3' adapter (5'-rAppAGATCGGAAGAGCGGTTCAGCAGGAATGCCGAG/3ddC/-3', 3ddC represented a 3' OH blocking group) that had an adenylated 5'-end and a ddC 3'-end was ligated to the 3' of the RNA using T4 RNA Ligase 2, truncated. The 5' adapter (5'-rArCrArCrUrCrUrUrUrCrCrCrUrArCrArCrGrArCrGrCrUrCrUrUrCrCrGrArUrCrU-3') ligation was performed using T4 RNA Ligase 1. The ligation product served as a template for cDNA synthesis using SuperScript II Reverse Transcriptase and an oligonucleotide with sequence complementary to 3' adapter as RT primer (5'-CTCGGCATTCTGCTGAACCGCTC-3'). The cDNA was amplified for 12 cycles using AccuPrime Pfx DNA Polymerase. The PCR product was purified on Novex 8% TBE polyacrylamide gel and the gel slice in the range of 140-190 nt was extracted and cleaned up by QiaQuick Gel Extraction Kit. Adapters and RT primer used in this study were purchased from Integrated DNA technology.

Illumina sequencing

The amplified library was measured using

quantitative PCR. RNA libraries were loaded into flow cell lanes at 8 pM concentration. mRNA and small RNA sequencing were carried out by running 38 and 76 cycles, respectively, on the Illumina IIG Genome Analyzer according to manufacturer's instructions.

Illumina Sequencing data analysis

Sequences were extracted from image files using the Illumina pipeline based on the default parameters of the pipeline. Single read sequences with read length 38 bp for mRNA and 76 bp for small RNA with high quality were obtained.

mRNA sequencing reads were screened for polymer, primer sequences, and ribosomal RNA sequences. The clean, high-quality sequencing reads were then mapped to human genome assembly (NCBI Build 37.1). The expression level was measured with reads per kilobase per million mapped reads (RPKM) by normalising the number of mapped reads to length of RNA and total number of mapped reads. The differential expression of genes was represented by fold change of RPKM of each gene in H1N1/H5N1 infected samples in response to mock. The heatmap of gene expression was generated based on hierarchical clustering of Log2 (fold changes) using MeV viewer v4.6.

Small RNA sequencing reads were trimmed with the low-quality ends (quality score=2) and primer adaptor sequences if more than 5 bp matched to the adaptor sequences. To quantify the trimmed sequencing reads, they were mapped to known miRNA database miRBase release 15. The abundance level of mature/mature* miRNA is represented by RPM (reads mapped per million mappable reads), where the mappable read counts normalised to the total number of mapped reads for each sample. In order to quantify the sequencing composition in the library, the remaining sequencing reads were aligned sequentially against known miRNA precursors, ribosomal RNA, tRNA (tRNA-SE), snoRNA (snoRNABase), and mRNA (NCBI RefSeq RNA release 39). Similar to the mRNA sequencing analysis, the relative abundance of miRNA is measured by fold change of RPM in H1N1/H5N1 infection samples in response to mock.

Pathway over-representation analysis

Pathway over-representation analysis was performed using the InnateDB platform (<http://www.innatedb.ca>). Over-representation analyses were performed using parameters (hypergeometric algorithm, Benjamini-Hochberg multiple testing correction). Results with corrected P values of ≤0.07 were considered statistically significant for mRNA pathways and ≤0.05 for miRNA target gene pathways. The choice of the P value was based on the conventional and empirical reasons such that the

significant and interested pathways were retained.

Results

Distinct cellular miRNA expression patterns in response to H1N1 and H5N1 influenza virus infection

The expression level of the known miRNAs in H1N1-, H5N1-, and mock-infected human macrophages at 1, 3, and 6 hours post-infection were compared. The proportion of sequence reads from each library that could be mapped to the miRBase 15, ranged from 19.13% to 32.08%. These mapped reads were from annotated known miRNAs as well as their precursor, mature, and mature star forms. The remaining sequence reads were derived from rRNAs, tRNAs, small snoRNAs, mRNAs, and the potential novel miRNA candidates. The relative abundance of miRNAs in each sample was measured with RPM by normalising against the different sequencing coverage depth of each sample. Compared with mock, the expression of miR-26b was apparently down-regulated in response to H1N1 and H5N1 infection at all time points. To investigate the differential expression of miRNAs in response to influenza A virus infection, the fold change of expression levels was calculated in influenza A virus infected cells and compared with mock-infected control cells. The miRNAs were ranked based on Z-statistics. The mature miRNAs with mappable reads >10 in at least one of nine sample datasets were included. Based on a fold change cut-off of 1.2, a total of 241 mature miRNAs were retained, and the differential expression pattern was revealed by the heat maps for H1N1- and H5N1-infected macrophages. From the mosaic structure of the heat maps, the altered expression trend in infection time and infection type was noted. Some miRNAs were up-regulated or down-regulated at all three time points and for both infection types. Many miRNAs had a similar time trend for H1N1 and H5N1 infection. However, several blocks of miRNAs behaved differently with time for H1N1 and H5N1 infection.

Based on a 1.2-fold cut-off, the differences in host response to H5N1 compared with H1N1 were determined. Most were co-regulated between H1N1 and H5N1 infection at 1, 3, and 6 hours. Respectively at 1, 3, and 6 hours after infection, 8, 4, and 5 mature miRNAs were up-regulated and 5, 7, and 22 mature miRNAs were down-regulated specifically in response to H1N1, whereas 6, 6, and 28 mature miRNAs were up-regulated and 14, 4, and 10 mature miRNAs were down-regulated specifically in response to H5N1. Notably, some were inversely regulated in response to H1N1 and H5N1 infection at the same time point. For example, compared with mock infection, miR-3123 was up-regulated (3.17 fold) after H1N1 infection and down-regulated (-1.84

fold) after H5N1 infection at 6 hours post-infection. It is believed that the differential expression for miRNAs correlates with that for their target genes.

The expression levels of selected miRNAs were verified using real-time PCR. Generally, all real-time PCR data correlated well with the RNA-Seq result.

Target genes of miRNAs and pathway analysis

The miRNAs with a fold-change of ≥ 1.2 and a Z-score of ≥ 3 were chosen for target prediction using DIANA-microT. Using the default setting of DIANA-microT, the target genes were obtained in response to H1N1 and H5N1 at each time point. The direction of expression (fold change ≥ 1.2) of target genes was inversely correlated with the expression of miRNAs. A list of miRNAs targeted genes was generated for pathway analysis using InnateDB.

Many pathways containing a number of genes targeted by differently expressed miRNAs were identified. For the 'RIG-I like receptor signalling pathway', there were 4 genes targeted by 7 up-regulated miRNAs and 9 genes targeted by 11 down-regulated miRNAs. Interestingly, in the 11 targeting down-regulated miRNAs, hsa-let-7 family has been verified to be tumour suppressor miRNAs responsible for regulating apoptosis in cell proliferation and developmental differentiation and involved in a feedback loop of MAPK signalling.³ hsa-miR-146a was recognised as innate immunity regulators acting as terminal transducers of TLR4 signalling and has been determined to target TRAF6 and IRAK1, whereas TRAF6 was also predicted to be targeted by hsa-miR-146a.⁴

Discovery of novel miRNA in human macrophages and influenza viruses

The sequencing reads falling into 'other' category, which could not be mapped to rRNA, tRNA, snoRNA, or mRNA, were used for computational detection of novel miRNAs for human mRNA-Seq. The un-mappable reads from each library (an average of 20% of the total reads) were aligned against human genome reference (GRCh37) for searching and determination of the potential loci of the hairpin sequences using the package miRDeep.⁵ A total of 43 novel miRNAs were identified to be potentially novel across the nine samples falling into 33 non-redundant groups. This was because the identical or highly similar mature miRNAs may be located on distinct hairpin loci. Those miRNAs were the potential homologous miRNAs.

Among the 43 novel miRNA candidates, 'AAAGAGCTTGGTCTTTGGAGCCA' was represented in all nine libraries with a maximum score of 2.4. 'CCTCAGAAACGCACCTGTTCCCTG' and 'GGCTCCACCTTCCTAGGTTGGC' were represented in eight of the nine libraries with a maximum

score of 2.1. The three candidates were considered to be highly confident and will be further studied in future. Other novel miRNA candidates were represented in no more than five libraries with the score varying between 0~4.2.

Discussion

This study investigated the miRNA expression profile in macrophages infected with H1N1 and H5N1 at 1, 3, and 6 hours post-infection. The differences in expression level of miRNAs may contribute to the differential gene expression observed in influenza virus-infected human macrophages. Thus, the miRNA and mRNA datasets were overlaid to identify the key regulatory mechanisms/networks involved in influenza pathogenesis.

This study identified many pathways/genes that are targeted by differently expressed miRNAs in response to H5N1 or H1N1 virus infection. In response to H5N1 infection, the RIG-I like receptor signalling pathway was the most significantly enriched pathway regulated by miRNAs.

This study identified differentially expressed known and novel miRNA, mRNA, and signalling pathways in response to influenza infection. Further

study should focus on these potential targets for drug development.

Acknowledgement

This study was supported by the Research Fund for the Control of Infectious Diseases, Food and Health Bureau, Hong Kong SAR Government (#08070532).

References

1. Wang TT, Parides MK, Palese P. Seroevidence for H5N1 influenza infections in humans: meta-analysis. *Science* 2012;335:1463.
2. Lee SM, Gardy JL, Cheung CY, et al. Systems-level comparison of host-responses elicited by avian H5N1 and seasonal H1N1 influenza viruses in primary human macrophages. *PLoS One* 2009;4:e8072.
3. Boyerinas B, Park SM, Hau A, Murmann AE, Peter ME. The role of let-7 in cell differentiation and cancer. *Endocr Relat Cancer* 2010;17:F19-36.
4. Bellon M, Lepelletier Y, Hermine O, Nicot C. Deregulation of microRNA involved in hematopoiesis and the immune response in HTLV-I adult T-cell leukemia. *Blood* 2009;113:4914-7.
5. Friedlander MR, Chen W, Adamidi C, et al. Discovering microRNAs from deep sequencing data using miRDeep. *Nat Biotechnol* 2008;26:407-15.

H5N1 virus resistant to antiviral drug

HL Chen *, Y Guan

KEY MESSAGES

1. This study investigated the geographical distribution and growth properties of avian influenza A (H5N1) isolates with mutations that confer resistance to amantadine and rimantadine. It also explored whether naturally occurring mutations associated with resistance to oseltamivir are present at a low frequency in H5N1 isolates and if so, whether these quasi-species may be the source of the emergence of oseltamivir-resistant strains following exposure to this drug.
2. Naturally occurring avian H5N1 virus mutants

resistant to the main types of antiviral drugs were noted.

3. The fitness of these mutants in avian and mammalian hosts needs further investigation.

Hong Kong Med J 2015;21(Suppl 4):S12-3

RFCID project number: 06060582

HL Chen *, Y Guan

Department of Microbiology, Li Ka Shing Faculty of Medicine, The University of Hong Kong

* Principal applicant and corresponding author: hlchen@hku.hk

Avian influenza A (H5N1) virus is common in poultry and has caused sporadic human infections since 2003. Antiviral drugs are essential to contain and delay the spread of the virus. Nonetheless, resistance to the M2 ion channel blockers, amantadine and rimantadine, and the neuraminidase inhibitor—oseltamivir—have been detected in H5N1 virus.

Human infections with H5N1 virus were first documented in Hong Kong in 1997 and then in China in 2003. More than 500 human infections have been identified in 15 countries; over 50% of cases are fatal.¹

Currently available anti-influenza drugs (adamantanes, amantadine, and rimantadine) block the ion channel formed by the M2 protein of the influenza virus, as well as the neuraminidase inhibitors—oseltamivir and zanamivir.²

Resistance to amantadine and rimantadine has been detected in human influenza viruses, including the pandemic (H1N1) 2009 virus,³ and in avian H5N1 viruses isolated in Vietnam and Thailand in 2004 and 2005.⁴ Stockpiling of neuraminidase inhibitors, in particular oseltamivir, is recommended by the World Health Organization in response to a potential pandemic. The efficacy of oseltamivir in the treatment of H5N1 infection is not clear, and resistant variants have been identified in H5N1 human cases treated with oseltamivir.¹ Emergence of resistance to oseltamivir in seasonal H1N1 virus since 2007 suggests that the resistance mutation—His274Tyr—may occur naturally.⁵ This study aimed to investigate whether resistance to amantadine is also prevalent in H5N1 viruses, and whether mutations associated with oseltamivir resistance occur in avian H5N1 viruses.

Resistance to amantadine and rimantadine is

mainly found in H5N1 viruses circulating in Vietnam and Thailand during 2004 and 2005 (data not shown). The dual Leu26Ile and Ser31Asn mutations in the M2 gene are responsible for this resistance. In vitro, the dual Leu26Ile and Ser31Asn mutations confer a growth advantage to the H5N1 virus, especially at 40°C. This suggests a possible mechanism for the expansion of mutant viruses in poultry that have a higher body temperature than humans (Fig). Resistance to adamantanes is much less prevalent in H5N1 viruses circulating in Indonesia, the Middle East, and China. This suggests that these drugs may still have prophylactic and therapeutic value for the H5N1 virus.

Resistance to the neuraminidase inhibitor—oseltamivir—has been found in H5N1 viruses. It is not clear whether the mutation—His274Tyr—originated in patients during treatment or whether it is derived from an avian source. In 2002, a H5N1 isolate was found to contain the His274Tyr mutation and was resistant to oseltamivir. His274Tyr quasi-species in H5N1 virus isolates were examined to investigate whether the His274Tyr mutant virus might naturally occur at low levels mixed with wild type virus in H5N1 poultry infections (data not shown). The His274Tyr quasi-species were more frequently found in isolates from infected chickens than from other ducks and geese, but no geographical difference was noted. His274Tyr mutant H5N1 viruses exhibited host specificity. A distinctive interaction between the HA and the NA proteins in some H5N1 isolates may also result in reduced susceptibility to oseltamivir. The mechanism for the emergence of the dominant His274Tyr in H1N1 virus was investigated to understand the fitness of the NA gene in N1 subtype viruses.

Although vaccination is a principal defence against influenza, rapid vaccine development during a pandemic is challenging. Antiviral drugs play an essential role in the control of an outbreak, delaying virus spread, as well as preventing and treating disease. A clear profile of H5N1 resistance to anti-influenza drugs is not available, as studies are still in the animal phase.

Although amantadine-resistant viruses have been found in Asia, their distribution was geographically and temporally confined to Thailand, Vietnam, and Cambodia; most isolates from other places are sensitive to amantadine, as have been most avian H5N1 viruses detected since 2006. This apparent geographical disparity in the susceptibility of H5N1 isolates to amantadine is unknown. The distinct and conserved pattern of the paired Leu26Ile and Ser31Asn mutations suggests that the Thai, Vietnamese, and Cambodian viruses originated from a single virus introduced into or generated within the region. Dual Leu26Ile and Ser31Asn mutations are rare among other influenza A viruses. The high incidence of 26Ile and its exclusive association with 31Asn in H5N1 isolates suggest that viruses carrying the dual mutation were stably selected; no single 26Ile variants were detected.

Neuraminidase inhibitors are the first-line antivirals for a pandemic. Resistance to oseltamivir has been reported in human H5N1 isolates. Oseltamivir-resistant strains bearing the His274Tyr mutation are present at low levels within some H5N1 virus populations. Isolation of one resistant mutant strain from an infected chicken suggests that such naturally occurring mutants may become the main population if they gain growth fitness in the host. This assertion is supported by the spread of a seasonal H1N1 virus carrying the His274Tyr oseltamivir-resistance mutation since 2007. Naturally occurring His274Tyr mutations in the 2009 H1N1 virus were also characterised. It is important to closely survey genetic mutations associated with resistance to neuraminidase inhibitors in influenza A viruses, and to study the replication fitness of resistant variants.

Acknowledgement

This study was supported by the Research Fund for the Control of Infectious Diseases, Food and Health Bureau, Hong Kong SAR Government (#06060582).

References

1. Writing Committee of the Second World Health Organization Consultation on Clinical Aspects of Human Infection with Avian Influenza A (H5N1) Virus, Abdel-Ghaffar AN, Chotpitayasunondh T, et al. Update on avian influenza A (H5N1) virus infection in humans. *N Engl J*

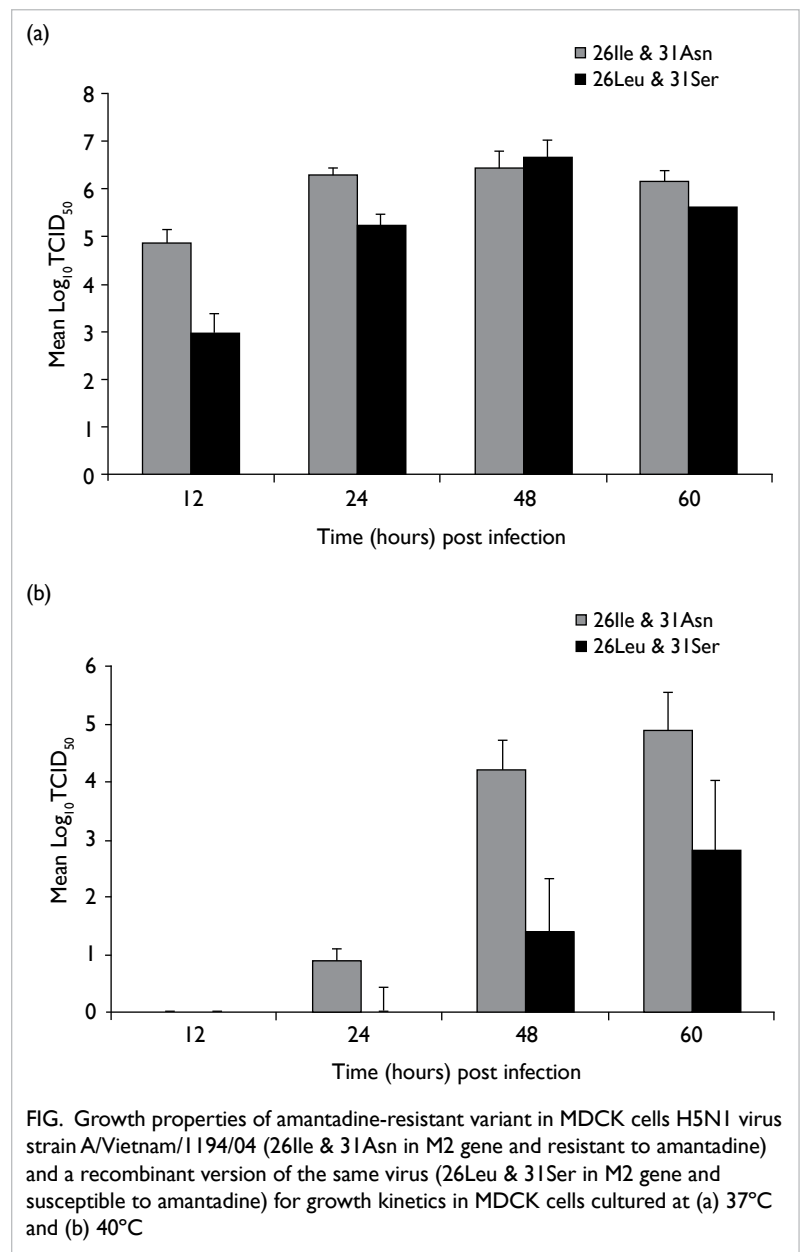


FIG. Growth properties of amantadine-resistant variant in MDCK cells H5N1 virus strain A/Vietnam/1194/04 (26Ile & 31Asn in M2 gene and resistant to amantadine) and a recombinant version of the same virus (26Leu & 31Ser in M2 gene and susceptible to amantadine) for growth kinetics in MDCK cells cultured at (a) 37°C and (b) 40°C

Med 2008;358:261-73.

2. Hayden FG. Antivirals for influenza: historical perspectives and lessons learned. *Antiviral Res* 2006;71:372-8.
3. Moss RB, Davey RT, Steigbigel RT, Fang F. Targeting pandemic influenza: a primer on influenza antivirals and drug resistance. *J Antimicrob Chemother* 2010;65:1086-93.
4. Cheung CL, Rayner JM, Smith GJ, et al. Distribution of amantadine-resistant H5N1 avian influenza variants in Asia. *J Infect Dis* 2006;193:1626-9.
5. Hauge SH, Dudman S, Borgen K, Lackenby A, Hungnes O. Oseltamivir-resistant influenza viruses A (H1N1), Norway, 2007-08. *Emerg Infect Dis* 2009;15:155-62.

Live recombinant *Salmonella* oral vaccine against avian influenza viruses

JD Huang *, BJ Zheng, KY Yuen

KEY MESSAGE

A live recombinant *Salmonella* oral vaccine platform against avian influenza viruses was constructed.

Hong Kong Med J 2015;21(Suppl 4):S14-6

RFCID project number: 07060572

¹ JD Huang *, ² BJ Zheng, ² KY Yuen

¹ Department of Biochemistry, The University of Hong Kong

² Department of Microbiology, The University of Hong Kong

* Principal applicant and corresponding author: jdhuang@hku.hk

Introduction

In 1997, the avian influenza virus (AIV) subtype H5N1 was first reported to infect humans.¹ Up to 3 March 2015, the cumulative number of confirmed human cases of H5N1 was 784, with 429 deaths. There is no evidence that H5N1 viruses can transmit efficiently from person to person.² Therefore, the key to prevention of a human H5N1 pandemic is to first control the H5N1 virus in birds.

Traditionally, inactivated influenza vaccines have been used prophylactically against pandemic influenza. However, their cost is high and yield is low, and they are difficult to administer on a large scale. The use of live, attenuated *Salmonella* vaccines has been extensively studied. *Salmonella* is a Gram-negative, intracellular bacterium.³ It has advantages as a live antigen delivery vector.⁴ First, it can be modified to express a wide range of antigens. Second, live *Salmonella* vaccine is easy to administer; it can be mixed with food and given to birds orally. Third, after oral administration, *Salmonella* can penetrate the Peyer's patches via M cells in the gastrointestinal tract and colonise the mesenteric lymph nodes that contain various antigen-presenting cells.³ This can generate a range of immune responses, including mucosal and systemic immunity. Fourth, live *Salmonella* vaccine can be easily and cheaply produced.⁵

This study constructed analogous sets of live recombinant *Salmonella* Typhimurium vaccine strains expressing a model antigen—enhanced green fluorescent protein (EGFP). The advantages and deleterious or synergistic effects of these vaccine strains were identified by comparing their immunogenicity in mice.

Methods

To develop an effective, live recombinant *Salmonella* oral vaccine against avian influenza viruses,

EGFP was used as a model antigen to study the relationship between immunogenicity and different antigen expression systems in *Salmonella*. Six 'single-recombinant' strains were constructed: three cytoplasmic expression strains based on a high or low copy plasmid, or the chromosome expression cassette (HP, LP and CP); two outer-membrane expression strains developed from a high copy plasmid or chromosome (HO, CO); and one eukaryotic expression plasmid, strain E. Several different pairs of EGFP-expression systems were combined to produce five additional 'double-recombinant' strains. The antigen expression levels, and immunogenic properties of these single and double-recombinant strains were systematically investigated in mice.

Based on the study of *Salmonella*-EGFP strains, three *Salmonella*-AIV strains were constructed: one chromosome-based *Salmonella* AIV strain (YBS010), in which multiple antigens of AIV (HA, NA, M2, NP) were inserted into the chromosome of *Salmonella* typhi Ty21a using an optimised recombinant method; one high-copy-plasmid-cytoplasmic-expression strain (C-HAOP); and one high-copy-plasmid-outer-membrane expression strain (O-HAOP). Their immune responses in mice and chicken were investigated via ELISA, ELISpot, haemagglutinin inhibition (HAI), and H5N1 virus challenge.

Results

Six 'single-recombinant' and five 'double-recombinant' *Salmonella*-EGFP strains were constructed to compare the immunogenic properties of various recombinant *Salmonella* strains. Maintaining high antigen expression levels was important for eliciting a strong B cell response. If the antigen (such as EGFP) is soluble and easily expressed in *Salmonella*, a low-copy plasmid-based strategy should be used, as it can provoke both

strong B cell and T cell responses. Furthermore, the stability of antigen expression is important for eliciting a strong T cell response against the recombinant vaccine strains. If a T cell response is preferred, a eukaryotic plasmid, or chromosome-based expression strategy may achieve better results. Nonetheless, a combination of two expression strategies did not enhance the immune response.

Based on the study of *Salmonella*-EGFP strains, three live recombinant *Salmonella* oral vaccine candidates against AIV were constructed. A chromosome-based *Salmonella* AIV strain YBS010 was first constructed. In the YBS010 strain, four antigen genes of AIV (HA, NA, M2, NP) were cloned and recombined into the chromosome of *Salmonella* typhi Ty21a strain using the novel recombinant method,⁶ and their expression was confirmed. Immunogenicity assays in mice (ELISA and ELISpot) indicated that they were not strong enough to generate protective B cell and T cell responses against the AIV (data not shown). According to the study of *Salmonella*-EGFP strains, a weak B cell response may be due to the low expression level of four antigens expressed by the single copy chromosome-based expression cassettes. A low T cell response was probably due to codon bias or inability to express soluble, correctly folded epitopes in YBS010.

Then, two *Salmonella*-HA strains were constructed including one cytoplasmic expression strain (C-HAOP) and one outer-membrane expression strain (O-HAOP). Both strains are based on high-copy plasmids. Previous studies have reported that many antigens from eukaryotic viruses (such as the HA protein from H5N1) cannot be readily expressed in a soluble form within the cytoplasm of *Salmonella*. Thus, the codons of the HA epitope were first optimised according to the *Salmonella* codon bias. Nonetheless, codon optimisation did not solve the insolubility problem of the HA epitope in C-HAOP strain. This may account for failure of the following immune test in mice models.

According to our in vivo immune response assays, no detectable B cell or T cell responses were observed when mice were immunised with the C-HAOP strain (Table 1). For O-HAOP strain, the use of the Lpp-ompA system resulted in the successful export of the HA epitope to the outer membrane fraction. Results from ELISA, HAI, and ELISpot assays in mice indicated that this strain was capable of inducing better HA-specific B cell and T cell responses than the corresponding C-HAOP strain (Tables 1 to 3) that expresses the HA antigen in the cytoplasm. The use of the Lpp-OmpA system probably helped the HA protein fold into a soluble conformation, or resulted in the export of increased amounts of HA protein, causing notable enhancements in immunogenicity. Although the

TABLE 1. HA-specific IgG responses in infected mouse sera

Group	No. responding / total No. (mean IgG titre)		
	Day 7	Day 28	Day 42
O-HAOP	1/10 (100)	3/10 (160)	3/10 (250)
C-HAOP	0/6 (0)	0/6 (0)	0/6 (0)

TABLE 2. Haemagglutinin inhibition (HAI) in infected mouse sera

Group	No. responding / total No. (mean titre)		
	Non-infection	HO	O-HAOP
O-HAOP	1/10 (100)	3/10 (160)	3/10 (250)

TABLE 3. IFN-γ responses to recombinant SL7207-HA strains

Group	Mean ratio (total mice No.)
HO	0.69 (n=5)
O-HAOP	2.56 (n=5)
C-HAOP	0.91 (n=5)

TABLE 4. HA-specific IgY responses in infected chicken sera

Group	No. responding / total no. (mean titre)		
	HO (1011)	O-HAOP (1010)	O-HAOP (1011)
Titre	0/4 (0)	0/4 (0)	0/4 (0)

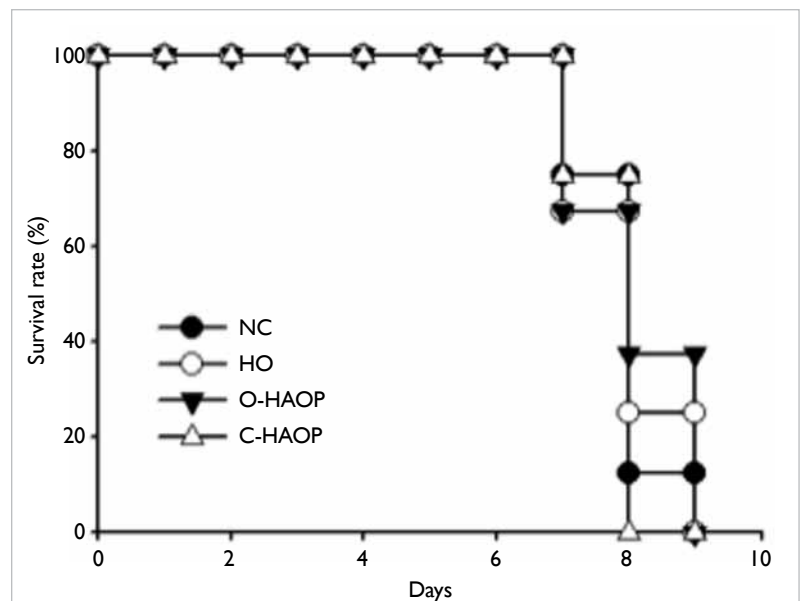


FIG. Challenge result of mice infected with C-HAOP and O-HAOP strains using the dose of 50 LD₅₀ H5N1 virus. Mice immunised with the HO strain and non-infected mice were negative controls. Mice were observed for sick and survival rates for 21 days. The survival rate per day after challenge was the challenge result.

O-HAOP strain increased the immune response in mice, this strain was still not strong enough to protect mice from the H5N1 virus challenge (Fig). In the chicken humoral immune response study, O-HAOP strain could not induce the significant HA-specific IgY response (Table 4). This may be due to the drawback of outer-membrane expression system in *Salmonella*-EGFP strains.

The total amounts of antigen synthesised and exported to the outer membrane were low, and the high-copy plasmid was not as stable as low-copy plasmid or chromosome-based expression cassette. Therefore, optimisation of this vaccine candidate is needed. Recombinant flagella can remain at the site of administration for many hours and are efficiently presented to the immune system to provoke the production of specific antibodies against the inserted foreign antigen and protection against challenge infection. The optimised recombinant technology can be used to integrate multiple copies of HA epitope into the *Salmonella* flagellin gene (*fliC*) to create a chromosome-based SL7207-*fliC*-HA strain. Chromosome-based expression cassette was more stable than plasmid-based expression cassette, which could help the flagellin-HA gene express constitutively. Flagellin-fused HA repeats would solve the insolubility problem of HA in the C-HAOP strain (cytoplasmatically expressed HA strain) and result in an increased expression level of HA compared with O-HAOP (outer membrane fused HA). The live, chromosome-based SL7207-*fliC*-HA strain could be orally administered to mice and chicken to test its immunogenic efficiency as described before.

Discussion

A method to integrate and express multiple H5N1 antigen genes in *Salmonella* was developed. It can serve as a general approach for future construction and optimisation of *Salmonella* recombinant strains.

The construction strategies of recombinant *Salmonella* vaccine strains for various needs and different forms of antigens were proposed. Such information can help guide the development of live recombinant *Salmonella* oral vaccines against AIV as well as other pathogens. If an epidemic arises,

relevant vaccines can be synthesised in a very short time.

Using the optimised recombinant method, several live *Salmonella* vaccine candidates against AIV were tested in animal models. These candidate vaccines stimulated a specific immune response against H5N1, although the efficacy was too low to protect the animals. Further optimisation of the vaccine candidates is necessary for rapid production during an epidemic. If AIV drifts or shifts to other subtypes, relevant vaccines can also be produced quickly.

As the vaccine can be administered orally, it is more convenient for mass administration in the poultry industry and avoids the use of hypodermic needles. The *Salmonella*-based vaccines also have the advantage of being easy to manufacture, as bacterial cultures need simple media and do not require special equipment.

Acknowledgement

This study was supported by the Research Fund for the Control of Infectious Diseases, Food and Health Bureau, Hong Kong SAR Government (#07060572).

References

1. Lipatov AC, Smirnov IuA, Kaverin NV, Webster RG. Evolution of avian influenza viruses H5N1 (1997-2004) in southern and south-eastern Asia [in Russian]. *Vopr Virusol* 2005;50:11-7.
2. Peiris JS, de Jong MD, Guan Y. Avian influenza virus (H5N1): a threat to human health. *Clin Microbiol Rev* 2007;20:243-67.
3. Ravindran R, McSorley SJ. Tracking the dynamics of T-cell activation in response to *Salmonella* infection. *Immunology* 2005;114:450-8.
4. Matic JN, Terry TD, Van Bockel D, et al. Development of non-antibiotic-resistant, chromosomally based, constitutive and inducible expression systems for aroA-attenuated *Salmonella enterica* Serovar Typhimurium. *Infect Immun* 2009;77:1817-26.
5. Shata MT, Stevceva L, Agwale S, Lewis GK, Hone DM. Recent advances with recombinant bacterial vaccine vectors. *Mol Med Today* 2000;6:66-71.
6. Yu B, Yang M, Wong HY, et al. A method to generate recombinant *Salmonella typhi* ty21a strains expressing multiple heterologous genes using an improved recombineering strategy. *Appl Microbiol Biotechnol* 2011;91:177-88.

The role of cathelicidin in control of *Helicobacter pylori* colonisation in the stomach

CH Cho *, J Yu, L Zhang, WKK Wu

KEY MESSAGES

1. A new animal model for *Helicobacter pylori* infection in the stomach was established.
2. A probiotic was transformed with a host defence peptide cathelicidin. This preparation can be used for the treatment and prevention of *H pylori* infection and gastritis.
3. This oral biological preparation can also be used for the treatment of ulcerative colitis. It has multiple actions including anti-inflammatory, anti-bacterial, and maintenance of the defence

mechanisms in the gastrointestinal mucosa.

Hong Kong Med J 2015;21(Suppl 4):S17-9

RFCID project number: 08070402

¹ CH Cho *, ² J Yu, ¹ L Zhang, ³ WKK Wu

Faculty of Medicine, The Chinese University of Hong Kong:

¹ School of Biomedical Sciences

² Department of Medicine and Therapeutics

³ Department of Anaesthesia and Intensive Care

* Principal applicant and corresponding author: chcho@cuhk.edu.hk

Introduction

The effect of host factors on colonisation with *Helicobacter pylori* remains poorly understood.¹ Cathelicidin is a pleiotropic host defence peptide responsible for the maintenance of innate immunity. In the stomach, the mature peptide is actively produced by surface epithelial cells, as well as chief and parietal cells, and is present in the gastric secretion. Consistent with its function as a host defence peptide, cathelicidin possesses microbicidal activity against a broad spectrum of microorganisms, such as bacteria and parasites. Mice that are deficient in cathelicidin are known to be more susceptible to necrotic skin infection caused by Group A *Streptococcus*.²

Cathelicidin is up-regulated in gastric secretion and epithelium inflamed by *H pylori* infection. In vitro, cathelicidin is bactericidal for several strains of *H pylori*, including SD4, SD14, and Sydney strain 1 (SS1), suggesting that it may play a role in protection against *H pylori* infection.³ Nevertheless, in vivo evidence of the effect of cathelicidin on *H pylori* colonisation is lacking. Study of *H pylori* infection in cathelicidin-knockout mice can help elucidate the role of cathelicidin in the control of *H pylori* colonisation in the stomach and protection against *H pylori*-induced chronic gastritis. The therapeutic potential of a bioengineered probiotic with the ability to actively secrete cathelicidin can be explored for its effect on bacterial colonisation and gastritis.

Methods

This study was conducted from December 2008 to June 2011. The *H pylori* standard strain SS1 was used. The *Lactococcus lactis* NZ3900 and plasmid pNZ8149 were purchased. *L lactis* was transformed

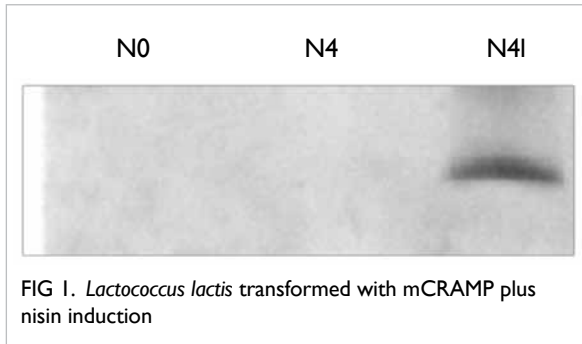
with pNZ8149-usp-Cath plasmid by electroporation as described previously.⁴ This plasmid contains secretion signal peptide usp45 and the nine-residue propeptides LEISSTCDA immediately upstream of mouse cathelicidin (mCRAMP). In the presence of the inducer nisin, mCRAMP is produced and secreted under the control of *nisA* promoter.

mCRAMP knockout (*Cnlp*^{-/-}) and 129/SVJ wild-type (*Cnlp*^{+/+}) mice were used. *Cnlp*^{-/-} and *Cnlp*^{+/+} mice were gavaged with either 10⁸ colony forming units (CFU) of *H pylori* SS1 or a sterile brain heart infusion broth (as a control) using gastric intubation needles every other day for a total of three doses.

Yellow colonies that formed on the Elliker agar were selected for PCR analysis. Positive clones containing recombinant plasmid gave the product size 712 bp, whereas the self-circulating vector had a band at 479 bp. Western blot revealed no bands in the *L lactis* (N0) and *L lactis* transformant without nisin induction (N4) groups. A clear band was noted at 4.7 kDa after nisin induction (N4I) [Fig 1].

In the treatment experiment, *L lactis* transformed with control plasmid (N) and mCRAMP-encoded *L lactis* (N4) were incubated in M17 broth with 0.5% lactose. Nisin (250 ng/mL) was added and further incubated for 3 hours (N4I). After *H pylori* infection for 1 month, the successfully infected *Cnlp*^{+/+} and *Cnlp*^{-/-} mice were randomised to one of three groups to receive (1) distilled water, (2) 10 log CFU of *L lactis* transformed with control plasmid (N), or (3) 10 log CFU of mCRAMP-encoded *L lactis* with the addition of inducer nisin (N4I). Oral administration was given every other day for 2 months.

In the pre-treatment experiment, both *Cnlp*^{-/-} and *Cnlp*^{+/+} mice were pre-treated with mCRAMP-



encoded *L lactis* and its control plasmid given once every 2 days for 2 weeks before *H pylori* challenge. They were then gavaged with either a 10⁸ CFU of *H pylori* SS1 or a sterile brain heart infusion broth (as a control) every other day for a total of three doses. The *H pylori* infected mice continued to receive either distilled water, 10¹⁰ CFU *L lactis* transformed with control plasmid, or 10¹⁰ CFU of mCRAMP-encoded *L lactis* with the inducer nisin for 3 hours. These animals were treated with these preparations every other day for 2 months.

The presence of *H pylori* and *L lactis* was shown by immunohistochemical staining. Rabbit anti-*H pylori* polyclonal and goat anti-*L lactis* polyclonal were used as primary antibodies,

respectively. Streptavidin-HRP conjugate was used as the secondary antibody for staining *L lactis*. The bacteria were visualised by diaminobenzidine chromogen. Goat antibody to mCRAMP was used as primary antibody. Alexa Fluor anti-goat 568 was used as secondary antibody. Sections were evaluated with a laser confocal microscope.

The relative density of *H pylori* was quantified by semi-quantitative PCR, detecting *H pylori*-specific 16S rDNA as previously described using specific primer HP5.⁵ The amount of mouse GAPDH DNA in the same specimen was measured for normalisation. The relative density of *H pylori* in the samples was expressed as the ratio of expression of *H pylori*-specific 16S rDNA to GAPDH DNA.

The RNA was used to generate the first strand of cDNA by reverse transcription. Specific primers were used to screen the expression of mCRAMP, TNF- α , IL-1 β , and IL-6.

The mucus layer was identified by periodic acid-Schiff staining. The mucus-containing cells were stained purple-red. The thickness of the mucus-secreting layer was measured perpendicularly to the mucosal surface from the edge of the epithelium to the outermost part of the mucus-secreting layer under microscopy. All analyses were performed blind.

Cultured 10⁸ CFU SS1 and 10783 *H pylori* were treated with 0.5, 1, 8, 64, and 128 μ g/mL mCRAMP,

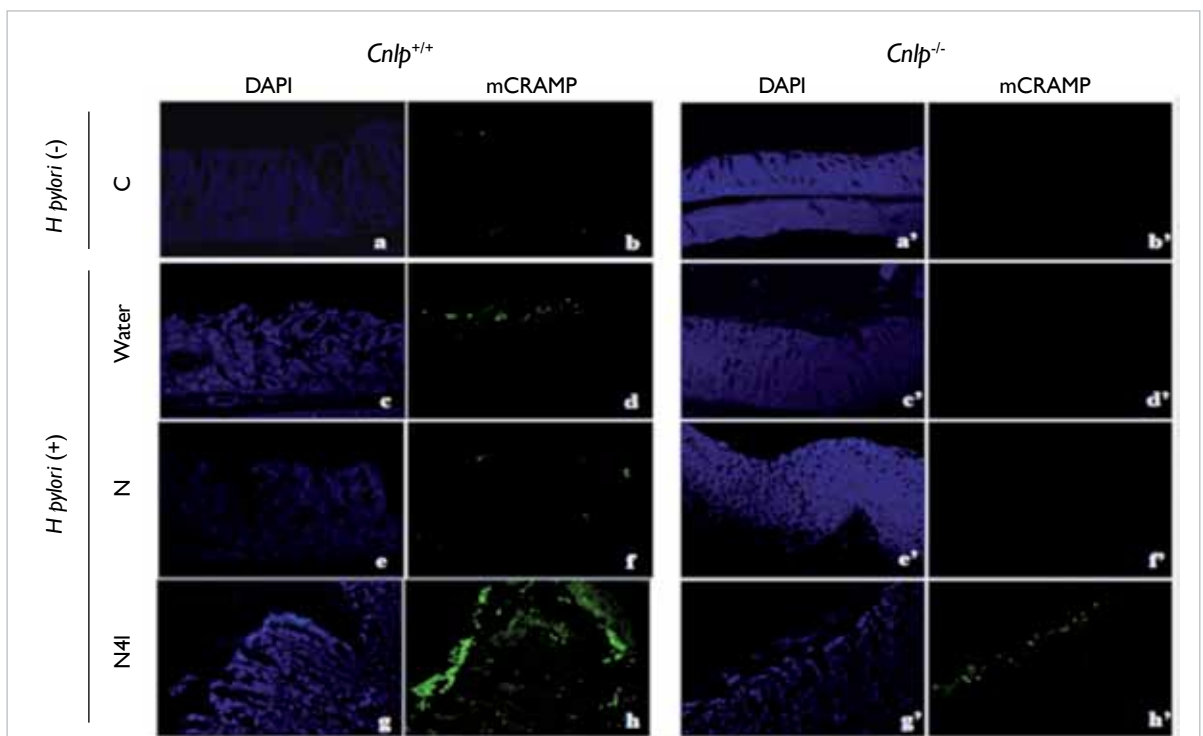


FIG 2. Immunofluorescent staining of mCRAMP in the stomach of *Cnlp*^{+/+} and *Cnlp*^{-/-} mice. Sections were stained with DAPI (blue) and antibody to mCRAMP (green). The present bioengineered probiotic preparation, the mCRAMP-encoded *L lactis* (N4I) successfully delivered exogenous mCRAMP to the gastric epithelium in the *Cnlp*^{+/+} and *Cnlp*^{-/-} mice. There was no staining of endogenous mCRAMP in *Cnlp*^{-/-} mice.

LL-37, LL17-32, or phosphate buffer saline as negative control. *H pylori* growth was determined by the OD595nm value of each well.

Acute ulcerative colitis was induced in mice by adding 3% dextran sulfate sodium to drinking water for 7 days.

Results

To assess whether *H pylori* and *L lactis* could colonise the surface of gastric epithelium in *Cnlp*^{+/+} and *Cnlp*^{-/-} mice, Giemsa and immunohistochemical stainings and scanning electron microscopy were performed. Both *H pylori* and *L lactis* were observed on the gastric mucosa of *Cnlp*^{+/+} and *Cnlp*^{-/-} mice after oral administration.

The mCRAMP level in the stomach was determined by immunofluorescence staining. In uninfected mice, gastric epithelial cells showed no mCRAMP expression. After *H pylori* infection, gastric epithelial cells stained positively for mCRAMP, suggesting that *H pylori* infection could induce mCRAMP expression in the gastric mucosa of *Cnlp*^{+/+} mice (Figs 2 d, f, and h). Oral administration of mCRAMP-encoded with *L lactis* successfully delivered mCRAMP to the gastric epithelium in both *Cnlp*^{+/+} and *Cnlp*^{-/-} mice (Figs 2 h and h').

Lack of endogenous mCRAMP increased *H pylori* infection and inflammation in the gastric mucosa. These pathological changes were prevented either by treatment or pre-treatment with cathelicidin-encoded *L lactis*.

The adherent mucus on the gastric mucosa was markedly depleted in gastritis mucosa. The effect was significantly prevented by the mCRAMP-encoded probiotic.

mRNA expressions of TNF- α , IL-1 β , and IL-6 were markedly increased by *H pylori* infection in both *Cnlp*^{+/+} and *Cnlp*^{-/-} mice. The increased levels were prevented by mCRAMP-secreting *L lactis*.

Cathelicidin and its analogues inhibited growth of normal and antibiotic-resistant strains of *H pylori*. Cathelicidin encoded *L lactis* prevented acute ulcerative colitis through multiple actions in mice.

Discussion

We have successfully established infection with *H pylori* in a new type of mice with genetic background of 129/SVJ. The infection was confirmed by immunostaining and electron microscopy of the gastric mucosa. This type of mouse model is useful to define the role of endogenous cathelicidin and also the therapeutic action of exogenous cathelicidin in *H pylori* infection and gastritis. We demonstrated for the first time that deficiency of cathelicidin (mCRAMP) can enhance *H pylori* infection and inflammation in the gastric mucosa. Supplementation

with a transformed probiotic *L lactis* with mCRAMP protected against *H pylori* infection and inflammation in the stomach. This is the first form of a biological preparation that combines a probiotic and a host defence peptide in a single preparation to prevent and treat *H pylori*. This mCRAMP encoded *L lactis* was shown to secrete mCRAMP both in vitro and in vivo. We also showed that human and mouse cathelicidin could not only eradicate the normal strain SS1 but also kill the clarithromycin resistant 10783 strain of *H pylori*. Moreover, the small fragment of human cathelicidin produces the best outcome to reduce bacterial growth. There are fewer side effects for this probiotic preparation, compared with the antibiotics conventionally prescribed for *H pylori* infection. This new form of preparation may provide a better option for the treatment of *H pylori* infection and its related diseases in murine animals, perhaps also in humans. To further extend the therapeutic application of mCRAMP-encoded *L lactis*, it was shown to be equally effective for murine UC, a disease related to bacterial infection. This biological preparation has several advantages over the prototype drug sulfasalazine. In addition to its anti-inflammatory action, it preserves the mucus level and maintains the integrity and function of the gastric mucosa. In conclusion, amalgamation of a probiotic with a host defence peptide is a good therapeutic agent for bacteria-associated diseases in the gastrointestinal tract.

Acknowledgements

This study was supported by the Research Fund for the Control of Infectious Diseases, Food and Health Bureau, Hong Kong SAR Government (#08070402), and a Direct Grant from The Chinese University of Hong Kong. We thank the Department of Microbiology, Prince of Wales Hospital for the help to culture *H pylori* in vitro.

References

1. Makola D, Peura DA, Crowe SE. *Helicobacter pylori* infection and related gastrointestinal diseases. *J Clin Gastroenterol* 2007;41:548-58.
2. Nizet V, Ohtake T, Lauth X, et al. Innate antimicrobial peptide protects the skin from invasive bacterial infection. *Nature* 2001;414:454-7.
3. Hase K, Murakami M, Iimura M, et al. Expression of LL-37 by human gastric epithelial cells as a potential host defense mechanism against *Helicobacter pylori*. *Gastroenterology* 2003;125:1613-25.
4. Holo H, Nes IF. High-frequency transformation, by electroporation, of *Lactococcus lactis* subsp. cremoris grown with glycine in osmotically stabilized media. *App Environ Microbiol* 1989;55:3119-23.
5. Roussel Y, Wilks M, Harris A, Mein C, Tabaqchali S. Evaluation of DNA extraction methods from mouse stomachs for the quantification of *H. pylori* by real-time PCR. *J Microbiol Methods* 2005;62:71-81.

Institutional risk factors for outbreaks of acute gastroenteritis in homes for the elderly: a retrospective cohort analysis

LW Tian *, WY Wong, SC Ho, S Ng, WM Chan

KEY MESSAGES

1. Norovirus is the major cause of acute gastroenteritis outbreaks in homes for the elderly in Hong Kong.
2. A larger home capacity and higher nursing staff-to-resident ratio were associated with increased outbreaks of acute gastroenteritis.
3. Installation of partitions between beds decreased the outbreaks of acute gastroenteritis.

Hong Kong Med J 2015;21(Suppl 4):S20-1

RFCID project number: 08070452

¹ LW Tian *, ² WY Wong, ¹ SC Ho, ³ S Ng, ³ WM Chan

¹ School of Public Health and Primary Care, Chinese University of Hong Kong

² Centre for Health Protection, Hong Kong SAR

³ Department of Health, Hong Kong SAR

* Principal applicant and corresponding author: linweit@hku.hk

Introduction

In 2006, 12.4% of the Hong Kong population were aged over 65 years. In 2005, about 60 000 elderly people were residents in homes for the elderly, accounting for 7% of this population. Infection is an important cause of mortality and morbidity in the institutionalised elderly.¹ Vulnerability of the elderly to infection and the living environment of homes for the elderly predispose to infection outbreaks.

Infection control programmes in health care facilities and their relation to infections have been reported.² This study aimed to investigate the association between institutional risk factors and outbreaks of acute gastroenteritis in homes for the elderly in Hong Kong.

Methods

This retrospective cohort study was conducted from August 2008 to February 2010. The cohort comprised 759 homes for the elderly; the outcome variable was the outbreak status of the homes; the homes that had multiple outbreaks of acute gastroenteritis within 2 months were considered once. The follow-up time was from 1 January 2005 to 31 December 2007. Information about the potential predictor variables, such as resident characteristics, staffing support and environment and facility conditions, was already available from the Territory-wide Infection Control Checklist Survey conducted by the Elderly Health Service of the Department of Health in the autumn of 2004. Outbreak data were extracted from the Public Health Information System.

Survival analysis for the homes for the elderly was performed; the endpoint was an outbreak. Cox

proportional hazard models were used to estimate the relative risk (RR) and 95% confidence interval (CI) for various variables. The method by Wei³ was used. Univariate analysis was performed for each potential variable. Variables with a P value of <0.1 were included in the multivariate Cox regression model.

Results

A total of 759 homes for the elderly and 57 522 elderly residents were included. There were 273 lab-confirmed outbreaks of acute gastroenteritis; the overall incidence was 12 outbreaks per 100 home-years. There were 3459 infected residents; the overall incidence was 2% per person-year. Of the 273 outbreaks, 262 (96%) were caused by noroviruses; thus analysis focused on norovirus outbreaks.

In univariate analysis, increased acute gastroenteritis outbreak rate was associated with larger home capacity, higher nurse-to-resident ratio, higher percentage of residents aged >75 years, less partition between beds, and better wheelchair accessibility. The RR for 30-resident per home increment, and 1/30 increment in nurse staff-to-resident ratio was 1.44 (95% CI, 1.36-1.53) and 1.2 (95% CI, 1.1-1.3), respectively.

In the multivariate Cox regression model, after adjusting for potential confounders, increased acute gastroenteritis outbreak rates were associated with better wheelchair accessibility (RR=1.7; 95% CI, 1.1-2.7), larger home capacity (RR=1.4; 95% CI, 1.3-1.5 for per 30 additional resident increment in one elderly home), higher nurse-to-resident ratio (RR=1.2; 95% CI, 1.1-1.3 for per 1/30 of ratio increment), and less partitions between beds (RR=0.6; 95% CI, 0.4-0.8).

Discussion

Our study found that the incidence of norovirus in residents of Hong Kong homes for the elderly was 2% per person-year, twice that of the general population.⁴ Noroviruses are a growing threat in the community and health care facilities,⁵ and can persist in the environment for a long time.

Homes with more residents had a higher probability of introducing pathogens from the community as well as transmitting them within the home. The relative difficulty of serving more residents within one home, as well as the increased person-to-person contact among residents, their relatives, visitors and staff with different characteristics, might create a higher chance of introduction and transmission of acute gastroenteritis outbreaks in larger homes compared with smaller ones.

Homes with more nurses had higher probably of bringing pathogens from the community. Another explanation may be attendant-borne transmission,⁶ in which attendants' hands serve as the vehicle to transmit institutional-acquired infections. Hand washing compliance in Hong Kong health care workers was low. Pathogens can be transmitted from immobile persons to nurses and health care workers and to other residents by direct contact or indirectly through their use of health care facilities. Pathogens can also be transmitted to the vulnerable elderly by attendants who were infected but remained asymptomatic.

Homes for the elderly with better wheelchair accessibility had an elevated risk of norovirus outbreaks. Wheelchairs may shorten the distance between ill residents and susceptible ones, and may encourage mixing of residents and physical contact among the elderly and between residents, health care workers and visitors.

Partition between beds was protective against outbreaks of norovirus. The partition could serve as a barrier to roommate transmission, decrease physical contact among the elderly, and thus diminish the possibility of transmission within a small room.

One limitation of the study was under-reporting. Generally, homes for the elderly report only serious infections; mild, self-limiting episodes of infection may not be reported. Nonetheless, laboratory confirmed outbreaks were used. Collection of information about exposure was

relatively objective and free from recall bias, and all homes for the elderly were included and thus free from selection bias.

Conclusions

Proper infection control measures are recommended, especially in homes for the elderly with larger capacity and more nurses, easy wheelchair access, and a high proportion of residents aged >75 years. Partitions should be installed between beds. Stricter health care procedures should be implemented.

Acknowledgements

This study was supported by the Research Fund for the Control of Infectious Diseases, Food and Health Bureau, Hong Kong SAR Government (#08070452). Ms Shelley Chan from the Department of Health helped with data cleaning and provided valuable advice in the data analysis and interpretation. Mr Hualiang Lin from The Chinese University of Hong Kong helped with the data cleaning, analysis and final report writing. Dr Krystal Lee and Prof SS Lee from The Chinese University of Hong Kong provided helpful comments on the study design, data analysis, and final report writing. We thank the Stanley Ho Centre for Emerging Infectious Diseases for supporting this study.

References

1. Jiang X, Turf E, Hu J, et al. Outbreaks of gastroenteritis in elderly nursing homes and retirement facilities associated with human caliciviruses. *J Med Virol* 1996;50:335-41.
2. Lopman BA, Andrews N, Sarangi J, Vipond IB, Brown DW, Reacher MH. Institutional risk factors for outbreaks of nosocomial gastroenteritis: survival analysis of a cohort of hospital units in South-west England, 2002-2003. *J Hosp Infect* 2005;60:135-43.
3. Wei LJ, Lin DY, Wiessfeld L. Regression analysis of multivariate incomplete failure time data by modelling marginal distributions. *J Am Stat Assoc* 1989;84:1065-73.
4. Ho SC, Chau PH, Fung PK, Sham A, Nelson EA, Sung J. Acute gastroenteritis in Hong Kong: a population-based telephone survey. *Epidemiol Infect* 2010;138:982-91.
5. Tsang OT. Nosocomial norovirus infection. *Bull Hong Kong Soc Infect Dis* 2007;11:2-7.
6. Godoy P, Artigues A, Bartolome R, Dominguez A, Plasència A. Norovirus gastroenteritis outbreak by person-to-person transmission in a nursing home [in Spanish]. *Med Clin (Barc)* 2006;127:538-41.

Liver cirrhosis–specific glycoforms of serum proteins in chronic hepatitis B infection: identification by lectin affinity chromatography and quantitative proteomic profiling

TCW Poon *, HLY Chan, HWC Leung, A Lo, RHY Lau, AY Hui, JJY Sung

KEY MESSAGES

1. Carbohydrate side-chains of serum glycoproteins are altered in patients with liver cirrhosis.
2. Sialylated and fucosylated variants of serum glycoproteins are altered in chronic hepatitis B (CHB) patients with liver cirrhosis.
3. Particular sialylated Hp variants are down-regulated in CHB patients with liver cirrhosis, as are in patients having liver cirrhosis secondary to chronic hepatitis C, non-alcoholic fatty hepatitis or autoimmune hepatitis.

4. Development of novel practical assays that can quantify a specific glycosylated variant of a particular serum glycoprotein is needed.

Hong Kong Med J 2015;21(Suppl 4):S22-6

RFCID project number: 04050392

TCW Poon, HLY Chan, HWC Leung, A Lo, RHY Lau, AY Hui, JJY Sung

Department of Medicine and Therapeutics, The Chinese University of Hong Kong

* Principal applicant and corresponding author: tcwpoon@cuhk.edu.hk

Introduction

In Hong Kong and China, chronic hepatitis B (CHB) is the commonest cause of liver cirrhosis, which is also a risk factor for development of hepatocellular carcinoma. In CHB patients, persistent hepatic inflammation leads to progressive liver fibrosis and subsequently cirrhosis. The process of liver cirrhosis is reversible. Accurate diagnosis is crucial for the management of CHB patients.¹ Liver biopsy is the gold standard for diagnosing cirrhosis, but is an uncomfortable and risky procedure. Therefore, serum markers for reliable detection of liver cirrhosis are needed.

Carbohydrate side-chains of serum glycoproteins are altered in patients with liver cirrhosis. Degrees of fucosylation on haptoglobin, alpha1-acid glycoprotein and cholinesterase increase in liver cirrhosis, but not in viral or chronic hepatitis.² Hyposialylated variants of haptoglobin, alpha1-antitrypsin, and transferrin are detected in patients with alcoholic cirrhosis.³

We developed a method to profile specific types of glycosylation variants of serum proteins by the combined use of lectin affinity chromatography and two-dimensional polyacrylamide gel electrophoresis (2D-PAGE).⁴ We aimed to identify serum glycoproteins as biomarkers of liver cirrhosis.

Methods

This study was conducted from 1 March 2006 to 31 August 2008. Patients with CHB who underwent

liver biopsies from 1998 to 2004 in the Prince of Wales Hospital were included. They were recruited or screened for previous and ongoing therapeutic trials or were suspected to have active liver disease on laboratory or radiological investigations. Serum samples were collected from 80 CHB patients with and without liver cirrhosis, and from 20 normal healthy subjects. In addition, 18 serum samples from patients with liver cirrhosis secondary to chronic hepatitis C (CHC) [n=10], non-alcoholic fatty liver disease (n=6), and autoimmune hepatitis (n=2) were examined. Serum samples were saved in a freezer (-80°C) for future study.

The serum samples were handled individually and subjected to differential lectin affinity chromatography to obtain glycoproteins fractions with altered glycosylation structures (including fucosylated N-glycan and sialylated N-glycan), which have been observed in CHB patients with liver cirrhosis or other chronic liver diseases. Fucosylated glycoproteins and sialylated glycoproteins were obtained by using LCA lectin and SNA lectin, respectively. The procedures were performed as previously described.⁴

The 2D-PAGE technology enabled differentiation of protein variants with various post-translational modifications.⁴ Isoelectric focusing (first dimensional separation by charge) of the proteins in the IPG strip was carried out in the PROTEAN IEF cell (Bio-rad). The IPG strip was then loaded on a SDS gel (PROTEAN II Ready Gel, Bio-rad) for second dimensional separation by protein

size. The gel images were subsequently analysed with the image analysis software PDQuest (Bio-rad). The samples were profiled in duplicate. The protein spots were matched and indexed across the 2D-PAGE images. The quantities of the protein spots were measured and normalised.

Protein identification was performed with some modifications.⁴ A protein spot was excised from the gel, destained and subsequently digested with trypsin. The masses of the recovered tryptic peptides were obtained by MALDI TOF/TOF mass spectrometer, and then compared to the masses of a peptide database calculated from the NCBI's nr

protein database. LIFT analysis was performed to obtain the amino acid sequence information of one or more tryptic peptides to confirm the protein identity.

Serum level of total Hp was measured by an in-house enzyme-linked immunosorbent assay (ELISA). Serum levels of s-Hp and ns-Hp were measured by combined use of a 96-well microtitre plate coated with SNA lectin, which captured alpha-2,6 sialylated glycoproteins, and a standard ELISA for Hp.⁴

The Mann-Whitney *U* test was used to compare differences between groups. The area under

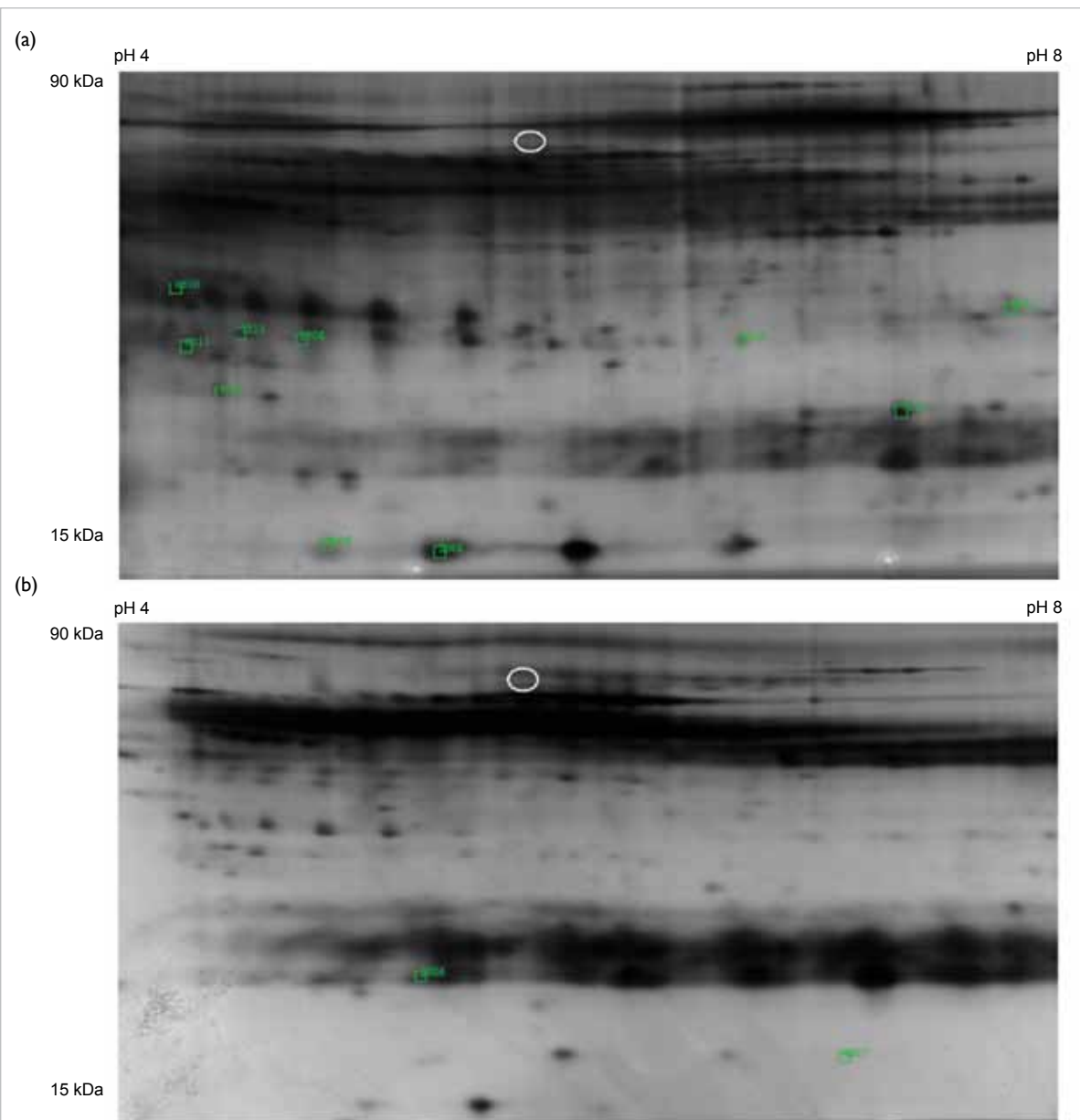


FIG. Representative images of (a) serum sialylated glycoproteins and (b) serum fucosylated glycoproteins purified by lectin affinity chromatography and subsequently resolved by two-dimensional polyacrylamide gel electrophoresis. The glycoprotein spots showing altered levels in chronic hepatitis B patients with liver cirrhosis are highlighted. White circles indicate the expected position (pI 5.8, 66.5 kDa) of albumin if present in the gel

the receiver operating characteristic (ROC) curve of a potential marker in the detection of liver cirrhosis was calculated according to standard formulae.

Results

Serum sialylated and fucosylated glycoproteins associated with liver cirrhosis

In CHB patients with liver cirrhosis, eight glycoprotein spots were down-regulated and two were up-regulated, compared to CHB patients without liver cirrhosis. All the 10 differential

glycoprotein spots showed a similar dysregulation trend in CHC patients (Fig a). Only two differential glycoprotein spots (SSP215 and SSP310) showed similar down-regulation patterns in patients with liver cirrhosis secondary to alcoholic cirrhosis or autoimmune hepatitis (Table 1). Of two glycoprotein spots (SSP2006 and SSP8005) up-regulated in the CHB patients with liver cirrhosis (Fig b), only one (SSP8005) showed the same up-regulation pattern as in patients with liver cirrhosis secondary to chronic hepatitis C infection, alcoholic cirrhosis or autoimmune hepatitis (Table 1).

TABLE 1. Serum sialylated and fucosylated glycoprotein spots that were significantly altered in chronic hepatitis B (CHB) patients with liver cirrhosis

Spot No.	Protein identity obtained by mass spectrometry		Mean (SD) normalised gel spot intensity					P value (2 tails)*
			Uniprot ID	Protein name	CHB patients without liver cirrhosis (n=40)	Patients with liver cirrhosis caused by		
	CHB (n=40)	Chronic hepatitis C (n=10)				Non-alcoholic fatty liver disease (n=6)	Auto-immune hepatitis (n=2)	
Sialylated glycoprotein spots								
SSP215	P10909	Clusterin, alpha chain	1264 (570)	773 (364)	685 (213)	1024 (714)	619 (8)	0.028
SSP310	P00738	Haptoglobin, beta chain	1061 (644)	698 (545)	802 (528)	886 (670)	464 (449)	0.041
SSP1101	-	-	797 (241)	559 (118)	593 (205)	923 (200)	684 (115)	0.023
SSP1313	P05156	Complement factor I	1535 (629)	958 (312)	1115 (474)	1408 (681)	833 (304)	0.009
SSP2008	P00738	Haptoglobin, alpha chain	7141 (8742)	2807 (1566)	5429 (4509)	6250 (3212)	8683 (6965)	0.029
SSP2009	-	-	1139 (1936)	259 (242)	692 (558)	553 (203)	2661 (716)	0.029
SSP2306	P00738	Haptoglobin, beta chain	1308 (709)	763 (283)	710 (553)	1322 (1003)	1317 (513)	0.043
SSP5206	-	-	456 (306)	196 (98)	216 (159)	600 (458)	196 (27)	0.029
SSP7112	-	-	2196 (566)	2828 (671)	2478 (565)	2621 (561)	2408 (86)	0.035
SSP8205	-	-	316 (122)	547 (172)	661 (216)	407 (42)	246 (179)	0.015
Fucosylated glycoprotein spots								
SSP2006	P01834	Ig kappa chain C region	1321 (237)	1621 (304)	1427 (500)	1137 (628)	815 (919)	0.016
SSP8005	P01620	Ig kappa chain V-III region	2814 (872)	5573 (4859)	4978 (3971)	4053 (1846)	4177 (1801)	0.016

* CHB patients with liver cirrhosis vs CHB patients without liver cirrhosis

TABLE 2. Serum levels of total Hp, ns-Hp, s-Hp, and s-Hp% in chronic hepatitis B (CHB) patients with or without liver cirrhosis

Marker	Healthy normal subjects (n=19)	CHB patients without liver cirrhosis (n=40)	Patients with liver cirrhosis caused by			Patients without liver cirrhosis (n=59)	Patients with liver cirrhosis (n=53)	P value (2 tails)*	
			CHB (n=40)	Chronic hepatitis C (n=9)	Non-alcoholic fatty liver disease (n=4)			Patients with CHB only	All patients
Mean (SD) total Hp (mg/mL)	1.01 (0.48)	1.46 (1.61)	0.75 (1.03)	1.52 (0.96)	2.79 (2.06)	1.23 (1.18)	1.04 (1.25)	0.038	0.073
Mean (SD) ns-Hp (mg/mL)	0.05 (0.04)	0.15 (0.15)	0.12 (0.17)	0.96 (1.44)	0.68 (1.19)	0.10 (0.12)	0.30 (0.74)	0.459	0.167
Mean (SD) s-Hp (mg/mL)	0.96 (0.50)	1.31 (1.56)	0.64 (1.02)	0.67 (0.56)	2.12 (2.41)	1.13 (1.16)	0.76 (1.17)	0.031	0.004
Mean (SD) s-Hp%†	87 (26)	77 (33)	64 (40)	53 (33)	51 (55)	82 (30)	61 (40)	0.253	0.006

* Patients with liver cirrhosis vs patients without liver cirrhosis

† s-Hp%=100% - ns-Hp%, where ns-Hp%=serum ns-Hp level/serum total Hp level x100%

Identities of the liver cirrhosis-associated serum glycoproteins

Among the 10 differential sialylated glycoprotein spots, protein identities of five down-regulated spots were obtained (Table 1). All identified glycoproteins were produced by the liver and secreted into the blood stream. The glycoprotein spots SS215 and SSP310 showing similar down-regulation patterns in all patients with liver cirrhosis (regardless of the pathogenesis) were clusterin and beta-chain of haptoglobin (Hp), respectively. For the two differential fucosylated glycoprotein spots (SSP2006 and SSP8005), they were in the immunoglobulin kappa chain C and V-III regions, respectively (Table 1). As immunoglobulin kappa chains did not carry any glycosylation, these two spots reflected up-regulation of fucosylated immunoglobulin variants in patients with liver cirrhosis.

Diagnostic value of sialylated haptoglobin in liver cirrhosis

In the 2D-PAGE image, four sialylated glycosylation variants of the alpha-chain of clusterin and 18 sialylated glycosylation variants of the beta-chain of Hp were found in patients with CHB. Among the 10 differential sialylated spots, two were the beta-chain of Hp, one was the alpha-chain of Hp, and one was the alpha-chain of clusterin. Therefore, sialylated Hp was more likely to be a useful marker for diagnosing liver cirrhosis. Subsequently, serum levels of total haptoglobin (total-Hp) [ie all haptoglobin variants regardless of glycosylation patterns], serum levels of sialylated Hp variants (s-Hp), and non-sialylated variants (ns-Hp) were measured. When comparing cases with and without liver cirrhosis, s-Hp ($P=0.004$) and s-Hp% ($P=0.006$) were significantly lower in the liver cirrhosis group (Table 2). When considering only the CHB patients, total-Hp ($P=0.038$) and s-Hp ($P=0.031$) levels were significantly lower in patients with liver cirrhosis (Table 2). This confirmed the results of the 2D-PAGE experiments, in which a sialylated variant of Hp was down-regulated in patients with liver cirrhosis, regardless of cause. Regrettably, ROC curve analyses showed that none of these markers were useful in differentiating cases with and without liver cirrhosis ($p>0.3$ in all instances).

Discussion

To the best of our knowledge, this is the first study providing concerted evidence that particular sialylated Hp variants were down-regulated in CHB patients with liver cirrhosis, as were in patients with liver cirrhosis secondary to CHC, non-alcoholic fatty liver disease or autoimmune hepatitis. The total-Hp level decreased (but not significantly) in patients

with liver cirrhosis, when all liver cirrhosis cases were considered. This was consistent with findings in a study in which the total-Hp level was not significantly decreased in chronic alcohol abusers.⁵

Differential lectin affinity chromatography and quantitative proteomic profiling were too complicated to be routine tests in chemical pathology laboratories. Thus, we examined the values of serum ns-Hp level, s-Hp level, and s-Hp% for diagnosing liver cirrhosis. Hyposialylated variants of haptoglobin were detected in patients with alcoholic cirrhosis.³ This was consistent with our finding that the ns-Hp% (which was equal to $100\% - s\text{-Hp}\%$), was significantly increased in patients with liver cirrhosis. Regrettably, ROC curve analyses showed that they were not useful markers. This was not unexpected, because only 2 of the 18 sialylated variants of the Hp beta-chain were down-regulated in patients with liver cirrhosis. The s-Hp level or s-Hp% were too crude to reflect the changes in these two variants.

Development of novel practical assays that can quantify a specific glycosylated variant of a particular serum glycoprotein is needed. We have developed a new method to quantify the N-glycans carried on Hp by the combined use of immunoprecipitation and linear MALDI-TOF mass spectrometry (unpublished data). We are developing a multiplex assay that can quantify the sialylated and/or fucosylated N-glycans on Hp, clusterin and immunoglobulin at the same time. With this novel assay, specific sialylated N-glycans and fucosylated N-glycans can be specific biomarkers for liver cirrhosis. Combined analysis of all the differential glycoforms or glycans of haptoglobin, complement factor I, and clusterin may help to improve the diagnosis of liver cirrhosis in CHB patients.

Conclusions

Using differential lectin affinity chromatography and quantitative proteomic profiling, altered levels of specific glycosylation variants of serum glycoproteins were identified in CHB patients with liver cirrhosis. Some of glycoproteins were produced by the liver and secreted into the blood stream. A sialylated Hp variant and a sialylated clusterin variant were down-regulated in CHB patients with liver cirrhosis, whereas fucosylated variants of immunoglobulin were up-regulated. Similar dysregulation trends were observed in patients with liver cirrhosis caused by CHC, alcoholic cirrhosis or autoimmune hepatitis. Decreased serum levels of s-Hp in patients with liver cirrhosis confirmed the proteomic profiling results. However, both serum s-Hp level and s-Hp% were not useful in the diagnosis of liver cirrhosis. Development of novel practical assays that can quantify a specific glycosylated variant of a particular serum glycoprotein is needed.

Acknowledgements

This study was supported by the Research Fund for the Control of Infectious Diseases, Food and Health Bureau, Hong Kong SAR Government (#04050392). We thank Li Ka Shing Institute of Health Sciences for providing support on research facilities.

References

1. Friedman SL. Liver fibrosis—from bench to bedside. *J Hepatol* 2003;38(Suppl 1):S38-53.
2. Ryden I, Pahlsson P, Lindgren S. Diagnostic accuracy of alpha(1)-acid glycoprotein fucosylation for liver cirrhosis in patients undergoing hepatic biopsy. *Clin Chem* 2002;48:2195-201.
3. Gravel P, Walzer C, Aubry C, et al. New alterations of serum glycoproteins in alcoholic and cirrhotic patients revealed by high resolution two-dimensional gel electrophoresis. *Biochem Biophys Res Commun* 1996;220:78-85.
4. Ang IL, Poon TC, Lai PB, et al. Study of serum haptoglobin and its glycoforms in the diagnosis of hepatocellular carcinoma: a glycoproteomic approach. *J Proteome Res* 2006;5:2691-700.
5. Chrostek L, Cylwik B, Krawiec A, Korcz W, Szmitkowski M. Relationship between serum sialic acid and sialylated glycoproteins in alcoholics. *Alcohol Alcohol* 2007;42:588-92.

Role of hepatitis B virus X protein in liver cancer

IOL Ng *, KMF Sze, GKY Chu

KEY MESSAGES

1. Full-length HBx and two natural C-terminal truncated HBx mutants (1-130 and 1-119 amino acid residues) do not alter the mitotic checkpoint control in hepatocytes or deregulate the expression of mitotic checkpoint proteins in hepatocellular carcinoma (HCC) cells.
2. The inducible gene expression systems are useful tools to characterise the role of HBx protein in

human HCC.

Hong Kong Med J 2015;21(Suppl 4):S27-30

RFCID project number: 05050022

IOL Ng *, KMF Sze, GKY Chu

Department of Pathology, Li Ka Shing Faculty of Medicine, The University of Hong Kong

* Principal applicant and corresponding author: iolng@hku.hk

Introduction

An estimated 350 million people worldwide are chronically infected with hepatitis B virus (HBV).¹ In Southeast Asia and Mainland China, including Hong Kong, the prevalence of HBV infection is high (10% in Hong Kong). Hepatocellular carcinoma (HCC) is a dreaded complication of chronic HBV infection; 55% of liver cancers worldwide occur in China including Hong Kong. HBV is a partial double-stranded DNA virus that comprises four known open reading frames: the viral DNA polymerase (P), viral envelope (surface antigens) proteins (PreS1, PreS2 or S), core protein (PreC or C), and HBV X protein (HBx). Among these four genes, HBx is the most frequently integrated and often considered an important factor in HBV-related hepatocarcinogenesis.² Integration of HBV DNA into the host genome is common in HCC and this may lead to alteration of the host cells by disrupting expression of cellular genes that are important for cell growth, survival, and cellular differentiation.^{3,4} Random HBV genome integration can also lead to truncation of the HBV genome, especially the HBx gene at the C-terminus.⁵⁻⁷ The function of HBx in HBV-associated HCC has been characterised, but its functional role in hepatocarcinogenesis remains unclear. This study aimed to (1) investigate the alteration by HBx of cell targets in HCC cells, (2) delineate the role of HBx in deregulation of mitotic checkpoint control, and (3) characterise the cellular effects of natural HBx mutants in HCC.

Methods

This study was conducted from September 2006 to August 2009.

In vitro functional characterisation of HBx in a HCC cell line and an immortalised normal liver cell line

Full-length HBx DNA (ayw subtype, GenBank No.:

U95551) was amplified from the HBx/pcDNA3.1+ plasmid⁸ and subcloned into Myc/pcDNA3.1+ and Myc/pLVX Tight Puro vectors. Two natural C-terminal truncation HBx mutants, HBxΔC1 (1 - 130 amino acid [aa]) and HBxΔC2 (1 - 119 aa) were generated and subcloned into Myc/pcDNA3.1+, Myc/pLVX Tight Puro, and Myc/pIND-Hygro vectors. Transient doxycycline- and ecdysone-inducible expression systems of full-length HBx, HBxΔC1 and HBxΔC2 were established for in vitro functional characterisation in the non-HBV infected immortalised normal liver cell line LO2 and HepG2 hepatoma cells.

RNA extraction and semi-quantitative RT-PCR

Total RNA was extracted from HCC cell lines using TriZOL (Invitrogen, Grand Island, NY, USA), according to the manufacturer's protocol. Primers for MAD1 (5'-CACCATGGTTTT ATCCACCC-3' and 5'-GCATCCAAGTTCTGCTGACA-3'), MAD2 (5'-CTTTTGTGTTTGTTG TCCCTGGC-3' and 5'-GTCATTGACAGGAATTTTGTAGG-3'), BUBR1 (5'- TGTAGCTCCGAGGGCAGG-3' and 5'-TTGAGAGCACCTCCTACACG-3'), BUB1 (5'-GTGGAGACATCCCATGAGGATC-3' and 5'-GGATCTTCTGCAATGGCAGCG-3') and BUB3 (5'-CGGGAAACGTTGCTTCTG-3' and 5'-TCTAGTCCCTCCACTCCAG-3') were used. β-Actin (primer set of 5'-GTGGGGCGCCCCAGGACACA-3' and 5'-CTCCTTAATGTCACGCACGATTC-3') was used as a reference for the amount of cDNA added in the PCR reactions.

Western blot analysis

Cells were lysed in sodium dodecyl sulphate-containing buffer and equal amounts of protein were separated on SDS-PAGE gel for western blot analysis. Immunodetection was performed using anti-c-Myc (Santa Cruz, CA, USA), anti-Flag (Sigma-

Aldrich, St Louis, MO, USA), anti-p53 (Santa Cruz), anti-p21 (Santa Cruz), anti-NF- κ B p50 (Santa Cruz), anti-NF- κ B p65 (Santa Cruz), anti-MAD1 (Bethyl Laboratories, Montgomery, TX, USA), anti-MAD2 (BD Transduction, San Jose, CA, USA), anti-BUBR1 (BD Transduction), and anti- α -tubulin (Sigma-Aldrich) antibodies.

Mitotic index measurement for analysis of mitotic checkpoint competence

Two $\times 10^5$ cells were seeded in six-well plates overnight and medium containing nocodazole at 0.2 μ g/mL or colcemid at 0.1 μ g/mL was applied to the cultures. Cells were collected at 24-hours, fixed in 3.7% of formaldehyde, stained with 4',6-diamidino-2-phenylindole (DAPI), and examined under an inverted fluorescence microscope. Cells with condensed nuclear DNA were considered as undergoing mitosis. To measure the mitotic index (percentage of viable cells arrested in mitosis), at least 300 cells were counted for each experiment using fluorescence microscopy. Data points represent the average results from two independent experiments. A cell line with mitotic index $<50\%$ following nocodazole or colcemid treatment was regarded as having mitotic checkpoint incompetence.⁹

Results

Inducible HBx-expression systems in HCC and immortalised normal liver cell lines

Transient overexpression of the full-length form of HBx (ayw subtype) caused a marked induction of cell death in the colony formation assay. Therefore, to stably express HBx for further functional studies, an inducible system—the doxycycline-inducible mammalian expression system—was used to study the effects of HBx. Adding doxycycline to the culture medium induced expression of the HBx protein in HepG2 and LO2 cells. The level of HBx expression closely correlated with withdrawal of doxycycline (data not shown). In addition, an ecdysone-inducible expression system was established in LO2 cells. Adding ponasterone A to the culture medium induced expression of HBx in LO2 cells. These inducible mammalian expression systems were useful to study the cellular effects of HBx.

Effect of full-length HBx on cellular targets, p53, p21 and NF- κ B, in HepG2 and LO2 cells

No significant change was noted in the protein expression of cell cycle regulators, p53 and p21/waf1/cip1, in HepG2 or LO2 cells with induced expression of full-length HBx. Similarly, there was no significant change in the protein expression levels of NF- κ B p65 or p50.

Effect of full-length HBx, HBx Δ C1 and HBx Δ C2 on mitotic checkpoint control

To determine whether HBx impaired mitotic checkpoint control, the mitotic checkpoint competence was examined by treating cells with either nocodazole or colcemid, both being microtubule-disturbing agents. A cell line with mitotic index $<50\%$ after nocodazole or colcemid treatment was considered to have mitotic checkpoint incompetence.⁹ There was no significant difference in the mitotic index between the LO2 cells stably expressing Myc-tagged full-length HBx and myc-tagged vector control (cell lines were treated with oxycycline for at least 7 days), indicating that full-length HBx had no significant effect on the mitotic checkpoint competence of LO2. There was also no significant difference in the mitotic checkpoint control in the presence of nocodazole or colcemid in LO2 cells expressing HBx Δ C1 or HBx Δ C2, compared with those expressing full-length HBx or vector control. These results suggest that the inducible expression of both full-length and C-terminal truncated HBx does not alter the mitotic checkpoint control of LO2 cells. As HepG2 cells were mitotic checkpoint incompetent,⁹ the mitotic checkpoint competence assay was not performed on HepG2 cells expressing the various forms of HBx.

Effect of full-length HBx, HBx Δ C1 and HBx Δ C2 on expression of mitotic checkpoint genes

To further investigate whether full-length HBx, HBx Δ C1, and HBx Δ C2 altered the expression of important mitotic checkpoint gene regulators (such as MAD1-3, BUB1, and BUB3), semi-quantitative RT-PCR and western blot analysis were performed. There was no significant change in expression at both mRNA and protein levels of MAD1, MAD2, and MAD3/BUBR1 in LO2 cells expressing full-length HBx, HBx Δ C1, or HBx Δ C2, compared with the vector control. There was also no significant difference in mRNA expression of other mitotic checkpoint genes, BUB1 and BUB3, LO2 cells expressing the various forms of HBx, compared with the vector control.

Discussion

HBV genomic DNA integration or mutation leads to COOH-truncation of the HBx protein in human HCC.^{5-7,10} COOH-truncated HBx DNA has been identified in 46% (23/50) of HBV-associated HCC tissue from HCC patients with chronic HBV infection.¹¹ About 79% of human HCCs from China have COOH-truncated HBx transcript in tumour tissue,⁵ suggesting that COOH-truncation of HBx is frequent in HCC in the Hong Kong population.

Cell invasiveness and up-regulation of uroplasinogen (uPA) is enhanced via NF-kappa B activation in HepG2 cells expressing full-length HBx.⁸ To determine whether HBx deregulated cellular targets in HCC, the protein expression of NF-κB and some cell cycle regulators (such as p53 and p21) were evaluated. There was no significant alteration in the expression of p53, p21, or NF-κB (p50/p65) when full-length HBx was expressed in HepG2 and LO2 cells with tetracycline inducible systems. Different subtypes or protein sequences of HBx can behave differently in repressing p21 protein expression in HCC cells¹²; the subtypes of HBx may be an influential factor.

DNA aneuploidy is frequent in human HCC.¹³ One of the leading causes of DNA aneuploidy is dysfunction of mitotic checkpoint regulation including alteration in abundance of mitotic checkpoint proteins or disruption of protein-protein interaction by viral proteins such as Tax protein in human T cell leukaemia virus type 1.^{9,14} In this study using Co-IP assays, full-length HBx interacted with the full-length form of MAD3/BUBR1 and p55cdc, but not with MAD1 or MAD2. As BUBR1 can interact with p55cdc when the mitotic checkpoint control is activated, we investigated whether the interaction between HBx and BUBR1 involved p55cdc, and a BUBR1 mutant, in which the putative p55cdc binding sites at BUBR1 protein were mutated, was constructed. The BUBR1 mutant could still interact with full-length HBx in the Co-IP assay, suggesting that HBx-BUBR1 interaction does not require the presence of p55cdc protein (data not shown). This is in line with a finding that HBx might alter the interaction between BUBR1 and p55cdc in mitotic checkpoint activation.¹⁵ Nonetheless, ectopic expression of HBx did not change the mitotic checkpoint status of LO2 cells, and the result differed from that observed in the HBx-expressing Chang liver cell line.¹⁵ Such discrepancy may be due to differences in the cell lines and the subtype of HBx (ayw subtype) used in the experiments.

To investigate the effect of C-terminal truncated HBx on mitotic checkpoint control, two natural C-terminal truncated forms of HBx found in human HCC were used: one with a breakpoint at 130 aa (HBxΔC1) and the other at 119 aa (HBxΔC2).^{5,7,16} Similar to full-length HBx, no significant difference was noted in the expression of mitotic checkpoint genes or alteration in mitotic checkpoint control in HBxΔC1- or HBxΔC2-expressing LO2 cells after treatment with nocodazole or colcemid. To determine whether HBx affects HCC tumour growth in nude mice, previous study has established full-length HBx stable knockdown cell in PLC/PRF/5 HCC cells and shown that knockdown of HBx inhibited HCC tumour growth.¹⁷ In our study, the HepG2 and LO2 cells with inducible expression of

full-length HBx and two truncated HBx forms were established to test the tumorigenicity in nude mice; neither HepG2 nor LO2 cells were tumorigenic. Therefore, the effect of C-terminal truncated HBx in tumour development requires further investigation using other cell line models. Our data suggested that neither full-length HBx (ayw subtype) nor natural C-terminal truncated HBx (1-130 and 1-119 amino acid) altered mitotic checkpoint control in hepatocytes.

Conclusions

Random HBV integration leads to C-terminus truncation of HBx in HCC. Our data suggest that neither full-length HBx (ayw subtype) nor natural C-terminal truncated forms of HBx (1-130 and 1-119 amino acid) alter the mitotic checkpoint control in hepatocytes or deregulate the expression of mitotic checkpoint proteins/genes in HCC cells.

Acknowledgements

This study was supported by the Research Fund for the Control of Infectious Diseases, Food and Health Bureau, Hong Kong SAR Government (#05050022). Part of the results of this study has been published in: Sze KM, Chu GK, Lee JM, Ng IO. C-terminal truncated hepatitis B virus x protein is associated with metastasis and enhances invasiveness by C-Jun/matrix metalloproteinase protein 10 activation in hepatocellular carcinoma. *Hepatology* 2013;57:131-9.

References

1. Lai CL, Yuen MF. Chronic hepatitis B--new goals, new treatment. *N Engl J Med* 2008;359:2488-91.
2. Feitelson MA, Duan LX. Hepatitis B virus X antigen in the pathogenesis of chronic infections and the development of hepatocellular carcinoma. *Am J Pathol* 1997;150:1141-57.
3. Wang J, Chenivresse X, Henglein B, Brechot C. Hepatitis B virus integration in a cyclin A gene in a hepatocellular carcinoma. *Nature* 1990;343:555-7.
4. Dejean A, Bougueleret L, Grzeschik KH, Tiollais P. Hepatitis B virus DNA integration in a sequence homologous to v-erb-A and steroid receptor genes in a hepatocellular carcinoma. *Nature* 1986;322:70-2.
5. Ma NF, Lau SH, Hu L, et al. COOH-terminal truncated HBV X protein plays key role in hepatocarcinogenesis. *Clin Cancer Res* 2008;14:5061-8.
6. Wang Y, Lau SH, Sham JS, Wu MC, Wang T, Guan XY. Characterization of HBV integrants in 14 hepatocellular carcinomas: association of truncated X gene and hepatocellular carcinogenesis. *Oncogene* 2004;23:142-8.
7. Tu H, Bonura C, Giannini C, et al. Biological impact of natural COOH-terminal deletions of hepatitis B virus X protein in hepatocellular carcinoma tissues. *Cancer Res* 2001;61:7803-10.
8. Chan CF, Yau TO, Jin DY, Wong CM, Fan ST, Ng IO. Evaluation of nuclear factor-kappaB, urokinase-type plasminogen activator, and HBx and their

- clinicopathological significance in hepatocellular carcinoma. *Clin Cancer Res* 2004;10:4140-9.
9. Sze KM, Ching YP, Jin DY, Ng IO. Association of MAD2 expression with mitotic checkpoint competence in hepatoma cells. *J Biomed Sci* 2004;11:920-7.
 10. Liu XH, Lin J, Zhang SH, et al. COOH-terminal deletion of HBx gene is a frequent event in HBV-associated hepatocellular carcinoma. *World J Gastroenterol* 2008;14:1346-52.
 11. Sze KM, Chu GK, Lee JM, Ng IO. C-terminal truncated hepatitis B virus x protein is associated with metastasis and enhances invasiveness by C-Jun/matrix metalloproteinase protein 10 activation in hepatocellular carcinoma. *Hepatology* 2013;57:131-9.
 12. Kwun HJ, Jang KL. Natural variants of hepatitis B virus X protein have differential effects on the expression of cyclin-dependent kinase inhibitor p21 gene. *Nucleic Acids Res* 2004;32:2202-13.
 13. Ng IO, Lai EC, Ho JC, Cheung LK, Ng MM, So MK. Flow cytometric analysis of DNA ploidy in hepatocellular carcinoma. *Am J Clin Pathol* 1994;102:80-6.
 14. Jin DY, Spencer F, Jeang KT. Human T cell leukemia virus type 1 oncoprotein Tax targets the human mitotic checkpoint protein MAD1. *Cell* 1998;93:81-91.
 15. Kim S, Park SY, Yong H, et al. HBV X protein targets hBubR1, which induces dysregulation of the mitotic checkpoint. *Oncogene* 2008;27:3457-64.
 16. Hsia CC, Nakashima Y, Tabor E. Deletion mutants of the hepatitis B virus X gene in human hepatocellular carcinoma. *Biochem Biophys Res Commun* 1997;241:726-9.
 17. Chan DW, Ng IO. Knock-down of hepatitis B virus X protein reduces the tumorigenicity of hepatocellular carcinoma cells. *J Pathol* 2006;208:372-80.

Viral mutant discovery in hepatitis B virus quasi-species in patients undergoing long-term lamivudine treatment

CM Ding, JJY Sung *, HLY Chan, J Luan

KEY MESSAGES

1. Matrix-assisted laser desorption ionisation time-of-flight mass spectrometry (MALDI-TOF MS) is an accurate method to detect drug-resistant mutations and identify novel mutations in chronic hepatitis B patients treated with lamivudine.
2. MALDI-TOF MS can simultaneously detect multiple mutations in a target sequence and at proportions as low as 10%.

Hong Kong Med J 2015;21(Suppl 4):S31-4
 RFCID project number: 07060222

CM Ding, JJY Sung *, HLY Chan, J Luan

Centre for Emerging Infectious Diseases, The Chinese University of Hong Kong

* Principal applicant and corresponding author: js_vcoffice@cuhk.edu.hk

Introduction

Hepatitis B virus (HBV) infection is a common cause of chronic hepatitis, liver cirrhosis, and hepatocellular carcinoma in Asia. The HBV reverse transcriptase lacks proof-reading activity. As a

result, it has a much higher error rate than DNA viral transcriptases, as it replicates through a RNA intermediate. HBV DNA is thus often present in quasi-species in an individual. One or more species may be favourably selected by factors such as host immune clearance and use of antiviral drugs.¹

HBV variation plays an important role in HBV genotypes and drug-resistant mutations. It is clinically important to detect known and unknown mutations that are associated with or conferred by drug resistance.² Current methods are insufficient to detect minor proportions of unknown mutants in an economic and efficient way. The most widely used method to detect novel mutants is direct sequencing. This provides complete sequence information, but it is not sufficiently sensitive for minor mutants present at <20% of the entire HBV population. Cloning and sequencing of virus sequences can also be used to detect minor mutations in HBV quasi-species, but it is costly, time-consuming, and labour-intensive.³ Thus, a high-throughput method for detecting virus mutations at minor proportions is needed. Matrix-assisted laser desorption ionisation time-of-flight mass spectrometry (MALDI-TOF MS) enables high accuracy, sensitivity and specificity. Some research groups have developed specific and sensitive assays based on this technology to detect known mutations.^{4,5}

This study evaluated the performance of base-specific RNA cleavage and MALDI-TOF MS in HBV from chronic hepatitis B (CHB) patients undergoing long-term lamivudine treatment.

Methods

This study was conducted from October 2007 to September 2009. A total of 195 serum samples from

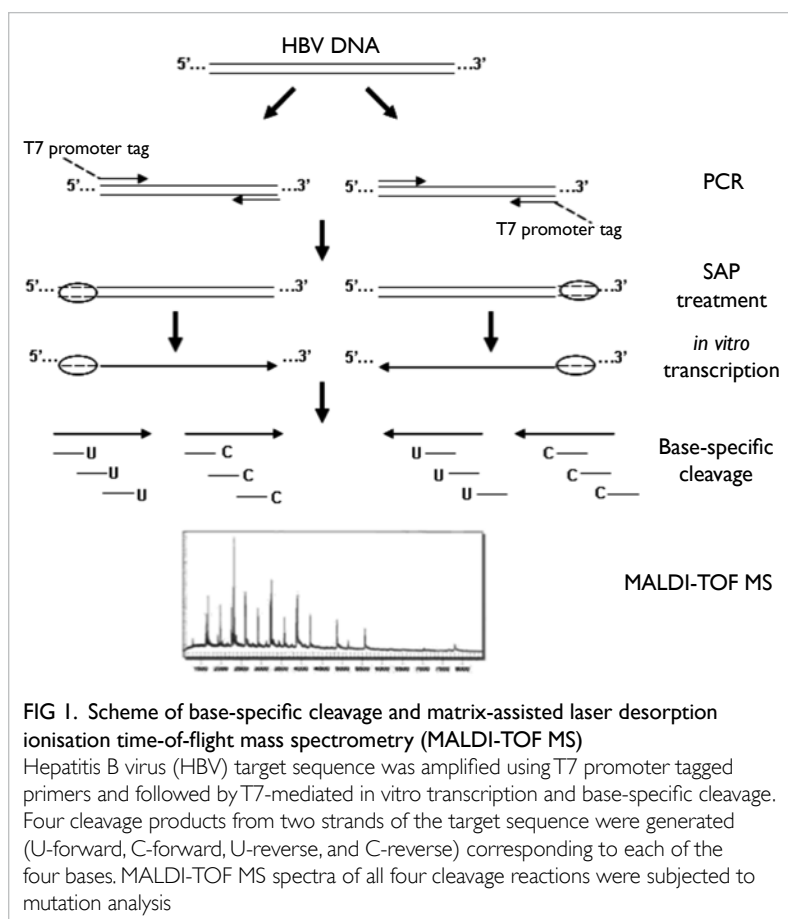


FIG 1. Scheme of base-specific cleavage and matrix-assisted laser desorption ionisation time-of-flight mass spectrometry (MALDI-TOF MS) Hepatitis B virus (HBV) target sequence was amplified using T7 promoter tagged primers and followed by T7-mediated in vitro transcription and base-specific cleavage. Four cleavage products from two strands of the target sequence were generated (U-forward, C-forward, U-reverse, and C-reverse) corresponding to each of the four bases. MALDI-TOF MS spectra of all four cleavage reactions were subjected to mutation analysis

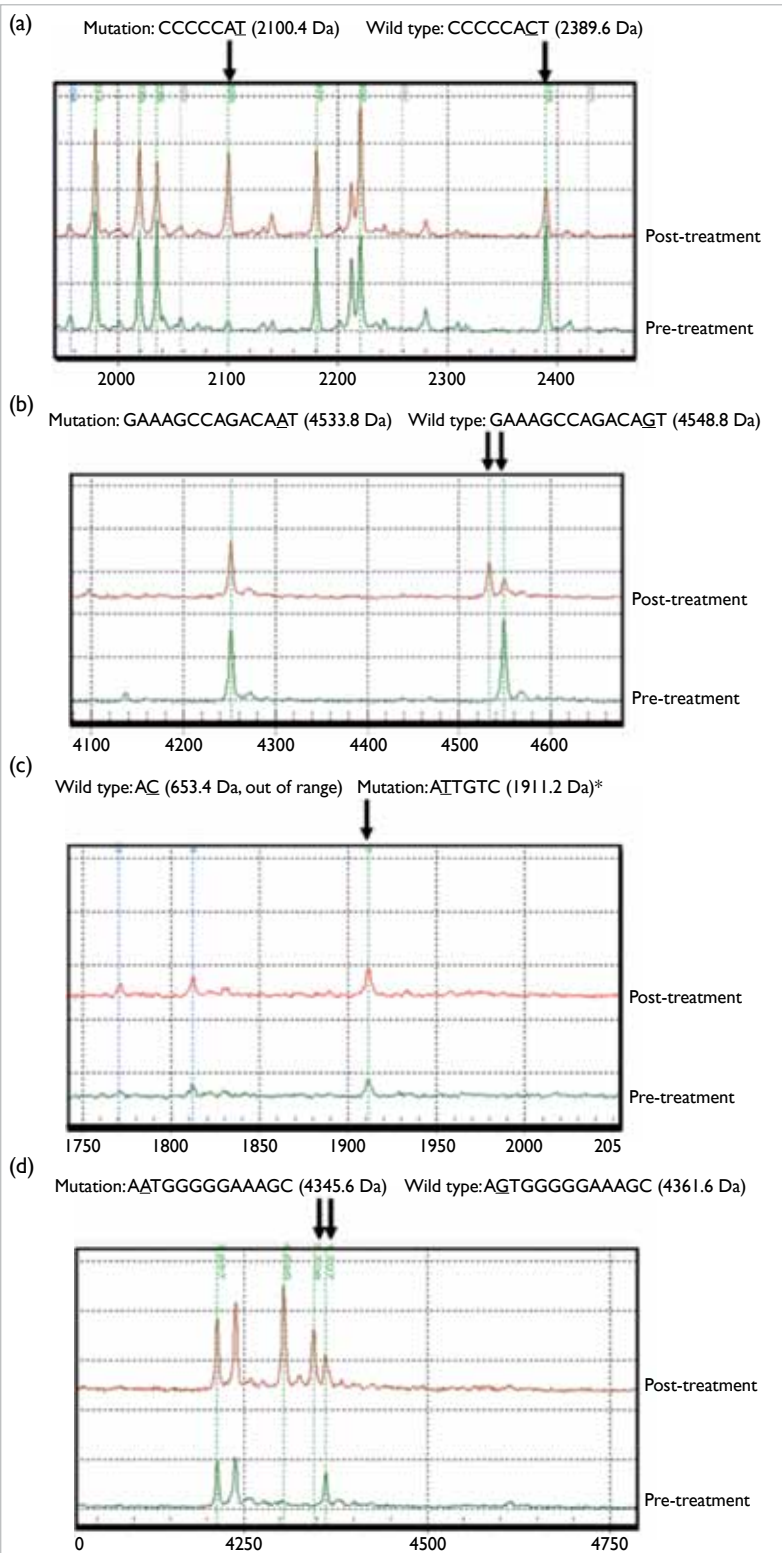


FIG 2. Matrix-assisted laser desorption ionisation time-of-flight mass spectrometry (MALDI-TOF MS) based discovery of a single mutation C/T@720 in hepatitis B virus (HBV) polymerase gene
 (a) In the T-specific cleavage of the forward RNA transcript, the C residue on the 2389.6 Da fragment was replaced by T, resulting in the presence of a new fragment (2100.4 Da). (b) In the T-specific cleavage of the reverse RNA transcript, the signal was shifted from 4548.8 Da to 4533.3 Da due to the replacement of C by T. (c) Signal changed at 1911.2 Da in the C-specific cleavage of the forward RNA transcript (* indicates the fragment shared the same compomer with others). (d) Mutation-specific signal at 4345.6 Da was observed in the C-specific cleavage of the reverse RNA transcript

30 CHB patients who received lamivudine treatment for 3 to 4 years, and 104 serial serum samples from 15 patients were analysed. For each patient, a pre-treatment sample and follow-up samples at 3-month intervals were collected. Mutations detected by MALDI-TOF MS were also studied by bi-directional sequencing and investigated randomly by cloning and re-sequencing.

Results and discussion

Base-specific RNA cleavage and MALDI-TOF MS

This new comparative approach combines the base-specific RNA cleavage reaction and automated MALDI-TOF MS analysis. HBV DNA sequence is amplified in two separate reactions that provide analysis for both strands (Fig 1). T7 promoter sequence tagged at the 5' end of the primer is incorporated into the target sequence during PCR reaction to initiate single-stranded RNA synthesis from the double-stranded PCR product via in vitro transcription. During in vitro transcription, deoxycytosine was used instead of cytosine (C), and thymidine (T) was substituted by uracil (U). Base-specific cleavage was achieved using RNase A, which ordinarily cleaves single-stranded RNA at each C or U residue. MALDI-TOF MS was applied to the products of each cleavage reaction and extracted a list of signal peaks with masses and intensities. Mass spectra obtained from four cleavage reactions were specific to each of the four bases of the target sequence.

Establishment of reference sequence

To monitor the nucleotide changes during antiviral treatment, the follow-up sequences of HBV isolated were compared with the sequence of HBV isolated before treatment. For each patient, the DNA sequence of the pre-treatment sample was obtained by directly sequencing PCR product using the primer pair of 683F and 915R and confirmed by another pair of primers (509F and 915R).

Detection of viral mutations in HBV quasi-species

After cleavage reactions, four characteristic patterns of fragments were generated and analysed by MALDI-TOF MS. Discovery of nucleotide changes was based on observing the changes in signal pattern by comparing measured spectra with an expected signal pattern predicted in silico from a reference sequence. Two types of signal changes indicate mutations: emergence of entirely new peaks and intensity change of existing peaks. The emergence of new peaks was the primary consideration for mutation identification because it displayed solid and reliable information on the new peak, whereas the

intensity change was used as supporting evidence. In addition, the surrounding sequence of mutations and concurrence of two mutations would affect the spectra and consequent analysis.

Detection of nucleotide change at position 720 of the HBV sequence in patient L011 was used as a demonstration. Figure 2a shows a portion of the spectrum ranging from 1960 Da to 2460 Da of T-specific cleavage of forward RNA transcript. The spectrum of the pre-treatment sample comprised seven expected signals, reflecting the fragments observed from the reference sequence. Comparison of the spectrum of the post-treatment sample with that of the reference sample yielded two observations: (1) a new signal represented a cleavage product with a composition of C5A1T1 (2100.4 Da), which was localised at position 38 of the amplicon (or nucleotide 720 of HBV sequence); (2) the intensity of the existing peak C6A1T1 (2389.6 Da) derived from the reference sequence decreased in the post-treatment sample. In the T-specific cleavage of reverse RNA transcript, partial replacement of wild type C by mutation T was confirmed. An additional peak at 4533.3 Da was detected while the signal intensity at 4548.8 Da was much lower in the post-treatment sample (Fig 2b). No informative signal could be obtained from the C-

specific cleavage of forward RNA transcript because the mutation-specific signal at 1911.2 Da of the post-treatment sample shared the same mass with other fragments in this reaction (Fig 2c). Confirmation was obtained in the spectrum of C-specific cleavage of the reverse transcript for the presence of a new peak at 4345.6 Da (Fig 2d).

The analysis of a mutation point was complicated by the presence and close proximity of a second mutation. For example, limited information could be obtained from the four cleavage reactions in identifying nucleotide changes at position 739 and 741 due to the nature of MassCLEAVE and detection range of MALDI-TOF MS. In addition, in some extreme cases, the detection of certain mutations was restricted by the surrounding DNA sequences.

Discovery of mutations in HBV quasi-species using MALDI-TOF MS and capillary sequencing

It is crucial to monitor the nucleotide changes and consequent amino acid substitutions during antiviral treatment. The baseline aminotransferase was 1135 IU/L and HBV DNA was $10^{8.2}$ copies/mL (Fig 3). Initial treatment with lamivudine had suppressed

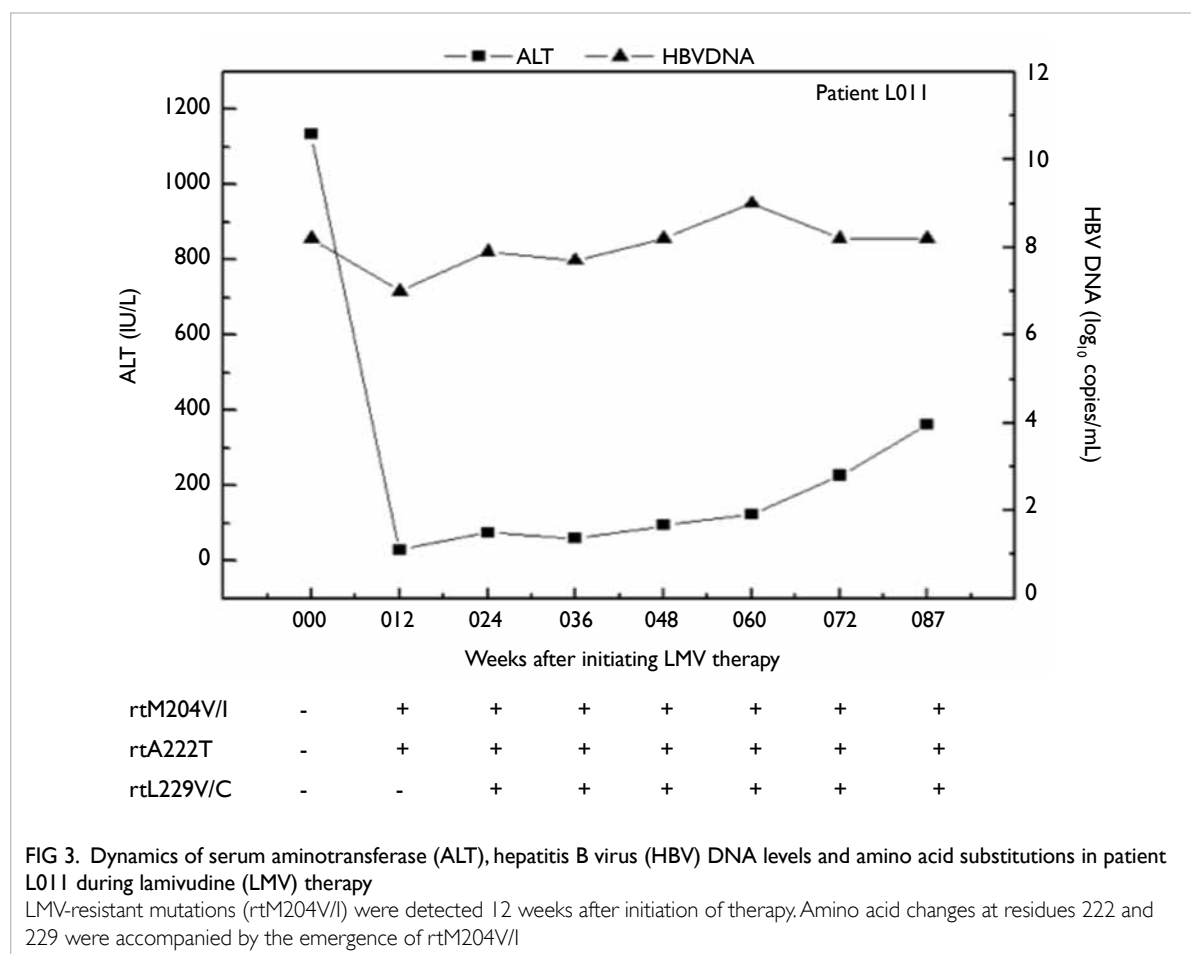


FIG 3. Dynamics of serum aminotransferase (ALT), hepatitis B virus (HBV) DNA levels and amino acid substitutions in patient L011 during lamivudine (LMV) therapy

LMV-resistant mutations (rtM204V/I) were detected 12 weeks after initiation of therapy. Amino acid changes at residues 222 and 229 were accompanied by the emergence of rtM204V/I

the viraemia, resulting in the decline of HBV DNA to $10^{7.0}$ copies/mL and serum aminotransferase to 30 IU/L after 12 weeks. Nonetheless, at follow-up time points, viral load had increased back to baseline levels. Seven out of eight samples at consequent time points showed lamivudine-resistant mutations—rtM204V and rtM204I. Additionally, amino acid changes at position 222 (rtA222T) and at position 229 (rtL229V/C) had been present along with the rtM204V/I mutations in this patient since 12 weeks. Early emergence of rtM204V/I was associated with lamivudine resistance, and other amino acid changes along with rtM204V/I may have contributed to antiviral treatment failure.

MALDI-TOF MS, combined capillary sequencing, offered such a high-throughput platform for discovering novel mutations. Its detection of multiple mutations in a single sample was generally good with up to eight mutations detected in patient L050. In addition, MALDI-TOF MS is cheap to perform (around US\$4 per sample for four cleavage reactions). Therefore, screening for potential mutations should be by MALDI-TOF MS for most samples, followed by confirmatory sequencing for special fragments in certain samples. This can be achieved with high efficiency and reduced cost.

Conclusions

MALDI-TOF MS is an accurate and cheap method

to detect novel viral mutations, and has a synergistic effect with capillary sequencing in identifying a minor proportion of viral quasi-species. Further studies of clinical and functional significance of the identified mutations are needed.

Acknowledgement

This study was supported by the Research Fund for the Control of Infectious Diseases, Food and Health Bureau, Hong Kong SAR Government (#07060222).

References

1. Torresi J, Locarnini S. Antiviral chemotherapy for the treatment of hepatitis B virus infections. *Gastroenterology* 2000;118(2 Suppl 1):S83-103.
2. Stuyver LJ, Locarnini SA, Lok A, et al. Nomenclature for antiviral-resistant human hepatitis B virus mutations in the polymerase region. *Hepatology* 2001;33:751-7.
3. Lok AS, Zoulim F, Locarnini S, et al. Antiviral drug-resistant HBV: standardization of nomenclature and assays and recommendations for management. *Hepatology* 2007;46:254-65.
4. Ding C, Chiu RW, Lau TK, et al. MS analysis of single-nucleotide differences in circulating nucleic acids: Application to noninvasive prenatal diagnosis. *Proc Natl Acad Sci U S A* 2004;101:10762-7.
5. Ding C, Wong VW, Chow KC, et al. Quantitative subtyping of hepatitis B virus reveals complex dynamics of YMDD motif mutants development during long-term lamivudine therapy. *Antivir Ther* 2006;11:1041-9.

Identification of hepatitis B virus DNA reverse transcriptase variants associated with partial response to entecavir

DKH Wong *, J Fung, CL Lai, MF Yuen

KEY MESSAGES

1. Entecavir is a potent antiviral agent against hepatitis B virus (HBV). In a cohort of 370 entecavir-treated chronic hepatitis B patients, 76 (21%) had a partial virological response, defined by detectable HBV DNA at year 1.
2. In HBV reverse transcriptase sequence analysis, 20 amino acid variants were identified solely in the partial responders.
3. There were 4 reverse transcriptase (rt) amino acid variants that had significantly different distribution between the optimal and partial entecavir responders.
4. HBV quasispecies complexity and diversity were

higher in the optimal responders than in the partial responders.

5. In multivariate analysis, high baseline HBV DNA, hepatitis Be antigen-positivity, and rt variant rt124N were significantly associated with partial entecavir response.

Hong Kong Med J 2015;21(Suppl 4):S35-8

RFCID project number: 08070852

DKH Wong *, J Fung, CL Lai, MF Yuen

Department of Medicine, The University of Hong Kong

* Principal applicant and corresponding author: danywong@hku.hk

Introduction

Nucleos(t)ide analogues (NA) are potent antiviral agents against hepatitis B virus (HBV) infection, drastically reducing viral load and improving clinical outcome. Lamivudine, adefovir, entecavir, telbivudine, and tenofovir are licensed in Hong Kong for treatment of chronic hepatitis B. Some patients have high HBV DNA, even at the initial stage.¹ One explanation is that some intrinsic viral properties may confer non-responsiveness to a particular NA. As the main target of NAs is HBV reverse transcriptase (rt), some natural polymorphisms in the HBV rt sequences may confer primary non-responsiveness.

HBV in a mixed viral population is known as quasispecies. Viral complexity and diversity change dynamically during the natural history of chronic hepatitis B infection. Studies of their effect on response to antiviral agents are rare. This study aimed to investigate whether there are some pre-treatment HBV rt sequence variations that predict response to entecavir. In addition, the association between quasispecies complexity and diversity and entecavir response were evaluated.

Methods

This study was conducted from May 2009 to November 2011. Between January 2002 and September 2009, 370 chronic hepatitis B patients at Queen Mary Hospital underwent daily entecavir (0.5 mg) therapy and were followed up for >1 year.

None had previously received NA or interferon/pegylated-interferon therapy. Patients with severe liver disease (chronic hepatitis C and autoimmune and alcoholic liver disease) were excluded.

Patient HBV DNA was measured at baseline and year 1 using the COBAS TaqMan HBV Test (Roche Diagnostics), with a lower limit and upper limit of detection of 60 copies/mL and 6.4×10^8 copies/mL, respectively. Optimal virological response was defined as profound HBV DNA suppression to ≤ 60 copies/mL at the end of the first year. Partial virological response was defined as a HBV DNA level of >60 copies/mL at year 1.

Baseline HBV rt sequence was amplified using a High Fidelity Taq Polymerase, followed by DNA sequencing. To identify sequence variants present at $<20\%$ in the viral population, HBV amplicons of the partial responders and randomly selected optimal responders were subjected to clonal sequencing. Differences in the pretreatment DNA polymorphism and HBV quasispecies complexity and diversity between the optimal and partial responders were noted.

Results

Baseline characteristics

Among the 370 (129 HBeAg-positive and 241 HBeAg-negative) patients, 76 (21%) exhibited a partial virological response to entecavir at year 1. Of these partial responders, 41% (53/129) were HBeAg-positive and 9.5% (23/241) were HBeAg-negative

($P < 0.0001$). The gender ratio, baseline alanine transaminase (ALT), albumin, and bilirubin levels were comparable between the optimal and partial responders (Table 1). The mean age was higher in the HBeAg-negative optimal responders than partial responders ($P = 0.026$). The partial responders had a higher baseline HBV DNA level than the optimal responders for HBeAg-positive ($P < 0.001$) and HBeAg-negative ($P = 0.001$) patients.

HBV rt sequence analysis

HBV rt DNA was successfully amplified by PCR in 305 patients (114 HBeAg-positive and 191 HBeAg-negative). Of these, 64 (21%) [47 HBeAg-positive and 17 HBeAg-negative] had a partial response to entecavir at year 1. For the partial responders, the

median HBV DNA level at year 1 was 639 copies/mL (range, $72\text{--}2.98 \times 10^7$ copies/mL), and the median baseline HBV DNA level was higher than that of the optimal responders (HBeAg-positive patients: 8.81 vs $7.83 \log_{10}$ copies/mL, $P < 0.001$; HBeAg-negative patients: 8.34 vs $6.62 \log_{10}$ copies/mL, $P = 0.001$).

Of the 344 amino acid residues in the HBV rt region, 217 were conserved among these 305 patients. Major known drug resistance mutations (rtL80I/V, I169T, V173L, L180M, A181V/T, T184G, A194T, S202I, M204I/V, N236T, and M250V) were not detected, except in one patient in whom concomitant rtL80I and rtL180M mutations were detected. Twenty amino acid variations (rt7D, rt7N, rt12Y, rt18K, rt53I, rt80I, rt118H, rt127W, rt128I, rt131S, rt135F, rt139Q, rt153W, rt180M, rt217R,

TABLE 1. Baseline characteristics of the optimal and partial entecavir responders

Characteristic	HBeAg-positive patients (n=129)			HBeAg-negative patients (n=241)		
	Optimal responders (n=76)	Partial responders (n=53)	P value	Optimal responders (n=218)	Partial responders (n=23)	P value
Mean±SD age (years)	42.6±12.3	40.7±10.8	0.36	51.3±9.3	46.8±8.4	0.026
No. of males:females	55:21	33:20	0.225	147:71	19:4	0.161
Median (range) hepatitis B virus DNA (\log_{10} copies/mL)	7.76 (4.40-8.81)	8.81 (5.41-8.81)	<0.001	6.43 (3.10-8.81)	7.64 (4.94-8.81)	0.001
Median (range) alanine transaminase (IU/L)	92.5 (12-2019)	107 (20-2144)	0.271	71.5 (11-3000)	93 (38-961)	0.133
Median (range) albumin (g/L)	42 (16-50)	42 (25-48)	0.657	42 (23-51)	42 (30-48)	0.763
Median (range) bilirubin (mmol/L)	14 (6-52)	12 (2-67)	0.162	11 (4-261)	14 (5-216)	0.086

TABLE 2. Distribution of reverse transcriptase (rt) polymorphisms found exclusively in partial responders receiving entecavir treatment for hepatitis B virus (HBV)

Gender	Age at baseline (years)	Baseline HBeAg status	HBV genotype	Baseline HBV DNA (copies/mL)	Year 1 HBV DNA (copies/mL)	rt variations exclusively found in partial responders
M	62.9	Positive	A	$>6.4 \times 10^8$	5.5×10^5	rt7D + 53I + 139Q + 153W + 217R
M	62.3	Negative	C	2.3×10^8	3.6×10^2	rt7N
F	53.8	Positive	C	$>6.4 \times 10^8$	4.4×10^3	rt12Y
M	22.3	Positive	B	1.0×10^8	1.6×10^2	rt18K
M	34.6	Positive	C	1.0×10^8	2.4×10^2	rt18K
M	48.2	Positive	C	1.1×10^8	2.1×10^2	rt80I + 180M
M	37.1	Negative	B	2.2×10^8	8.2×10^1	rt118H
M	28.7	Positive	B	$>6.4 \times 10^8$	1.3×10^3	rt127W
M	37.6	Negative	B	$>6.4 \times 10^8$	2.7×10^2	rt128I
M	45.7	Positive	B	$>6.4 \times 10^8$	2.3×10^2	rt131S
M	31.4	Positive	B	1.0×10^8	1.6×10^2	rt135F
M	51.8	Positive	C	8.0×10^6	2.1×10^3	rt153W
M	54.8	Negative	C	1.5×10^5	8.5×10^1	rt219T
F	52.5	Negative	B	$>6.4 \times 10^8$	4.5×10^2	rt233L
F	35.1	Positive	C	$>6.4 \times 10^8$	4.5×10^2	rt322I
M	22.0	Positive	C	1.0×10^8	5.1×10^4	rt329N
F	39.9	Positive	C	$>6.4 \times 10^8$	1.8×10^3	rt336Q

rt219T, rt233L, rt322I, rt329N, and rt336Q) were found exclusively in partial responders. These variations were distributed among 17 partial responders (Table 2). Variants rt18K and rt153W were found in two cases, and all other variants were found only once. Due to the rarity, association between these polymorphisms and partial/slow response was not significantly different and needed to be determined by phenotypic assays.

The distribution of some rt amino acid variations differed significantly between optimal and partial responders. Specifically, 17 amino acid variants were present at a significantly higher frequency in 64 partial responders than in the 241 optimal responders (Table 3). After controlling for false discovery during multiple comparisons using Bonferroni correction, four rt variants, namely rt 53N, rt118N, rt124N, and rt332S, remained to have a significantly higher frequency in the partial responders than in the optimal responders (Table 3).

Multivariate analysis was performed to determine the independent factors associated with partial entecavir response at year 1. All factors with significantly different distribution among the partial and optimal responders were analysed, namely baseline HBeAg status, age, HBV genotype, baseline HBV DNA level, rt53N, rt118N, rt124N, and rt332S (the four rt variants with differential distribution) (Table 3). Multivariate logistic regression analysis revealed that high baseline HBV DNA levels ($P < 0.0001$, OR=2.30, 95% CI=1.60-3.34), HBeAg-

positivity ($P < 0.001$, OR=3.68, 95% CI=1.79-7.62), and rt variant rt124N ($P = 0.001$, OR=3.09, 95% CI=1.54-6.18) were independently associated with suboptimal entecavir response at year 1.

Minor sequence variations identified by clonal sequencing

Clonal sequencing was performed on the 64 partial responders and 34 randomly selected optimal responders. Among the polymorphisms found exclusively in the partial responders (Table 2), the variant rt18K was detected as minor species in five additional cases, rt118H was detected in one additional case, rt128I in two additional cases, rt131S in four additional cases, rt135F in one additional case, and rt153W in one additional case.

HBV Quasispecies complexity and diversity

Quasispecies complexity and diversity were compared between the optimal and partial responders. The optimal responders had a higher quasispecies complexity (higher normalised Shannon entropy) than the partial responders at the nucleotide level ($P = 0.036$) and at the amino acid level ($P = 0.087$) [Table 4]. Similarly, the optimal responders had a higher quasispecies diversity than the partial responders (all $P < 0.05$, Table 4).

Discussion

Entecavir is a potent nucleoside analogue that

TABLE 3. Reverse transcriptase (rt) variants with significantly different distribution among partial responders and optimal responders

rt variant	% of variants found in partial responders	% of variants found in optimal responders	P value (unadjusted)	P value (after Bonferroni correction)
rt9H	68.8	53.0	0.025	1
rt16T	50.0	29.6	0.002	0.254
rt53N	51.6	27.4	0.00024	0.031
rt109S	54.7	35.3	0.005	0.635
rt118N	48.4	25.3	0.00034	0.043
rt121I	51.6	29.5	0.001	0.127
rt124N	50.0	23.7	0.000038	0.0048
rt127R	46.9	29.0	0.007	0.889
rt131N	50.0	28.2	0.001	0.127
rt134N	35.9	16.2	0.00048	0.061
rt151Y	51.6	30.3	0.001	0.127
rt221Y	53.1	37.8	0.026	1
rt222A	40.6	21.6	0.002	0.254
rt238H	50.0	31.1	0.005	0.635
rt271M	48.4	26.1	0.001	0.127
rt278V	70.3	54.8	0.025	1
rt332S	43.8	20.1	0.00010	0.013

TABLE 4. Quasispecies complexity and diversity of the entecavir optimal and partial responders

Quasispecies	Optimal responders (n=34)	Partial responders (n=63)	P value
Complexity: normalised Shannon entropy			
Mean (range) nucleotide level	0.9673 (0.6868-1)	0.9316 (0.3324-1)	0.036
Mean (range) amino acid level	0.8668 (0.4930-1)	0.7869 (0.2192-1)	0.087
Diversity			
Mean (range) genetic distance (nucleotide level) [10 ⁻³ substitutions]	8.7083 (3.2747-36.4403)	5.2904 (0.8906-56.1354)	0.019
Mean (range) genetic distance (amino acid level) [10 ⁻³ substitutions]	14.0147 (3.3561-66.2545)	8.6151 (0.8923-94.822)	0.032
Mean (range) No. of synonymous substitutions per site (10 ⁻³)	12.4076 (3.8811-42.0139)	7.4706 (0.6533-78.0112)	0.015
Mean (range) No. of non-synonymous substitutions per site (10 ⁻³)	6.6121 (1.6396-30.8776)	3.9649 (0.4040-43.8353)	0.039

suppresses HBV DNA replication. The present study showed that 21% of patients still had detectable HBV DNA after 1 year of therapy. HBV rt sequence analysis of 64 partial responders and 241 optimal responders showed that 20 HBV rt variants were present exclusively in partial responders. However, these variants occurred only in one or two cases, and the association was not significant. In addition to the 20 variants found solely in partial responders, four variants were present in a higher proportion in the partial responders than in the optimal responders. Multivariate analysis showed that high baseline HBV DNA, HBeAg-positivity, and the rt variant rt124N were independent factors associated with slow entecavir response. This is consistent with our previous study in which patients with positive HBeAg and HBV DNA of >8 log copies/mL had a lower rate of HBV DNA undetectability at year 1 to 3.¹ rt124N variant was associated with partial entecavir response, even though only 50% of the partial responders harboured this variant. Further long-term study is needed to demonstrate the possible role of rt124N and the variants identified solely in the partial responders in susceptibility to entecavir.

Two case reports have identified HBV rt variants S219A + Y245H and S246T in entecavir non-responders.^{2,3} Phenotypic assays determined that the rt variant pattern S219A + Y245H (rather than S246T) are associated with a lower susceptibility to entecavir in vitro. The present study did not identify S219A + Y245H variants. Nevertheless, the findings of rt124N and the 20 'unique' variants may provide a preliminary identification of putative variant pattern of reduced susceptibility to entecavir.

In the clonal sequencing data, the optimal responders had a significantly higher quasispecies complexity and diversity than the partial responders. It is possible that in the optimal responders a higher complexity and diversity was present. There may be a 'less-fit' subpopulation of viral quasispecies more susceptible to entecavir. In contrast, in the partial responders, the viral population was less diverse

and more replication competent, causing a slower entecavir response. Further studies using technology with a greater sequencing depth (such as ultra-deep pyrosequencing or next generation sequencing) are needed to further elucidate the association between quasispecies complexity/diversity and treatment response.

Conclusions

We identified 20 rt variants found exclusively in entecavir partial responders and four rt variants with significantly different distribution among the optimal and partial responders. High baseline HBV DNA levels, HBeAg-positivity, and rt124N were associated with partial entecavir response at year 1. The possible association between rt variants and entecavir response needs to be proved by in vitro phenotypic studies.

Acknowledgements

This study was supported by the Research Fund for the Control of Infectious Diseases, Food and Health Bureau, Hong Kong SAR Government (#08070852). We thank Dr Daniel Fong for his advice on statistical analysis. Results of this study have been published in: Wong DK, Kopaniszen M, Omagari K, et al. Effect of hepatitis B virus reverse transcriptase variations on entecavir treatment response. *J Infect Dis* 2014;210:701-7.

References

1. Yuen MF, Seto WK, Fung J, Wong DK, Yuen JC, Lai CL. Three years of continuous entecavir therapy in treatment-naive chronic hepatitis B patients: VIRAL suppression, viral resistance, and clinical safety. *Am J Gastroenterol* 2011;106:1264-71.
2. Karatayli E, Karatayli SC, Cinar K, et al. Molecular characterization of a novel entecavir mutation pattern isolated from a multi-drug refractory patient with chronic hepatitis B infection. *J Clin Virol* 2012;53:130-4.
3. Hu JL, Cui J, Guo JJ, et al. Phenotypic assay of a hepatitis B virus strain carrying an rtS246T variant using a new strategy. *J Med Virol* 2012;84:34-43.

Modulation of cytokine responses by adrenomedullin and adrenomedullin binding protein-1 in macrophages: a novel pathway in sepsis

LYF Wong, BMY Cheung *

KEY MESSAGES

1. Adrenomedullin augments the production of interleukin-10, a cytokine that limits inflammation.
2. Interferon- γ , a cytokine that is increased in inflammation, downregulates the receptor and binding protein of adrenomedullin.
3. Cyclic AMP mediates the increased expression of adrenomedullin, interleukin-6, and interleukin-10 in response to endotoxin.
4. The production of interleukin-6 is mediated by p38-mitogen-activated protein kinase (MAPK), p42/44-MAPK, protein kinase C, and protein kinase K, whereas that of interleukin-10 is mediated by p38-MAPK and protein kinase K.
5. These downstream pathways could be targets for therapeutic intervention.

Hong Kong Med J 2015;21(Suppl 4):S39-44

RFCID project number: 05050082

LYF Wong, BMY Cheung *

Department of Medicine, The University of Hong Kong

* Principal applicant and corresponding author: mycheung@hku.hk

Introduction

Polymicrobial sepsis is a life-threatening disorder. Patients die of septic shock and multiple organ failure caused by lipopolysaccharide (LPS) and other bacterial products. A hyperdynamic phase is followed by shock and circulatory collapse. Myocardial dysfunction frequently accompanies severe sepsis and septic shock secondary to circulating depressant factors, including tumour necrosis factor- α (TNF- α) and interleukin-1 beta (IL-1 β). Macrophages produce proinflammatory cytokines including TNF- α , IL-1 β , and IL-6 that lead to tissue injury.

Adrenomedullin (AM) is a vasorelaxant peptide originally isolated from the adrenal medulla. It relaxes vascular smooth muscle cells through the elevation of intracellular cyclic adenosine 3'-5'-monophosphate (cAMP).¹ It also acts on endothelial cells by activating adenylyl cyclase and nitric oxide synthase, resulting in dilation of blood vessels. The macrophage produces AM in inflammation and sepsis. Transgenic mice over-expressing AM are resistant to septicaemic shock. AM markedly increased IL-6 production in both resting and LPS-stimulated macrophages, but significantly suppressed LPS-induced TNF- α secretion.² IL-6 and IL-10 can inhibit the production of pro-inflammatory cytokines such as TNF- α and IL-1. These results suggest that AM may play an important role as an anti-inflammatory regulator

of the inflammatory response in the macrophages, at least partly, via its effect on production of inflammatory cytokines.

Elevated levels of AM play a major role in initiating the hyperdynamic response during the early stage of sepsis, yet transition to the late, hypodynamic phase occurs, despite continued high circulating levels of AM.³ A specific AM binding protein-1 (AMBP-1) carries AM in human plasma and is complement factor H.⁴ The decreased vascular response to AM in advanced sepsis is related to a decrease in AMBP-1. Administration of AM/AMBP-1 to septic animals prevents the drop in blood pressure and reduces mortality. AM and AMBP-1 in combination down-regulate pro-inflammatory cytokines in septic animals, and suppress LPS-induced TNF- α expression and release from the macrophages.⁵

The interaction between AM and AMBP-1 has opened a new avenue for research into the transition from the hyperdynamic to the hypodynamic phase of sepsis. AM has been reported to induce its effect through the cAMP-, Ca²⁺, or mitogen-activating protein kinase (MAPK) mediated pathway. Expression of AMBP-1 is detectable in both monocytes and macrophages, and AMBP-1 given in conjunction with AM further raises AM-induced cAMP production. Nonetheless, little is known about the regulation of AMBP-1, the cause of reduced AMBP-1 production in sepsis, or the regulatory

pathways involved to elicit the physiological actions of AM and AMBP-1.

The study aimed to (1) investigate the expression of AM, AMBP-1 and AM receptor proteins in the LPS-induced inflammatory response in a rat alveolar macrophage cell line; (2) examine the effect of AM and AMBP-1 on LPS-induced inflammatory cytokine production in macrophages and determine whether feedback loops or desensitisation of AM receptors affect the production of AM and AMBP-1; and (3) identify a potential role of second messenger-dependent kinases in the regulation of AM and AMBP-1 expression and AM-induced cytokine responses in LPS-stimulated macrophages.

Methods

This study was conducted from October 2006 to March 2008. NR8383 rat macrophages were stimulated by IFN- γ , TNF- α , IL-6, and IL-10 with or without LPS (at 1 to 1000 ng/mL) for 6 and 24 hours.^{2,6} Levels of AM, AMBP-1, and AM receptor proteins (calcitonin receptor-like receptor [CRLR]) and receptor activity-modifying protein (RAMP2 and RAMP3) mRNA were quantified using real-time PCR (ABI PRISM Sequence Detection System 7000, Applied Biosystems Group) or semi-quantitative RT-PCR after reverse transcription. Immunoreactive AM was measured by a radioimmunoassay (Phoenix Pharmaceuticals, Belmont, CA, USA).

NR8383 rat macrophages and human monocytic cell line THP-1 were studied. THP-1 cells were incubated with 100 nM phorbol 12-myristate 13-acetate (PMA, Sigma, USA) for 72 hours to induce differentiation into macrophage-like cells. The cells were stimulated by LPS (10 ng/mL) and AMBP-1 (500 nM) in the presence or absence of AM or AM receptor antagonists (AM₂₂₋₅₂ or CGRP₈₋₃₇) for 6 and 24 hours. Concentrations of TNF- α , IL-6, and IL-10 in the culture supernatants were measured using enzyme-linked immunosorbent assays (ELISA, R&D Systems, USA). To study desensitisation of the AM receptor, cells were pre-incubated with AM (1 to 1000 nM) for 2 hours followed by a washout period and a re-stimulation by LPS with or without AM/AMBP-1. The concentration of TNF- α , IL-6, and IL-10 in the supernatant was measured.

NR8383 macrophages were stimulated by LPS (10 ng/mL) with or without addition of AM, forskolin (an adenylyl cyclase activator), SQ22536 (Qbiogene, an adenylyl cyclase inhibitor) or dibutyryl-cAMP (a membrane permeable cAMP analogue) or a signalling pathway inhibitor for 6 and 24 hours. Inhibitors of protein tyrosine kinase (PTK) (genistein, Merck, USA), p38 and p42/44 MAPK, protein kinase A (PKA), and protein kinase C (PKC) were used. TNF- α , IL-6, and IL-10 in the supernatant were measured.

Changes in cytokine levels were analysed using

analysis of variance or t-test as appropriate. A P value of <0.05 was considered significant.

Results

Expression of AM, AMBP-1, and AM receptor proteins in the LPS-induced inflammatory response in a rat alveolar macrophage cell line

In unstimulated NR8383 cells, AMBP-1 was constitutively expressed, with a RT-PCR cycle threshold of 26.62 ± 0.08 compared with 18.35 ± 0.07 for β -actin. Basal mRNA expression of CRLR and RAMP-2 were low, with a mean RT-PCR cycle threshold of 30.77 ± 0.03 and 35.52 ± 0.07 , respectively, compared with 18.35 ± 0.07 for β -actin.

LPS increased expression of CRLR by 5- to 26-fold at 6 hours ($P < 0.01$), which declined to 5- to 11-fold above basal at 12 hours and to 2- to 4-fold above basal at 24 hours. IFN- γ , TNF- α , IL-6, or IL-10 had no effect on CRLR mRNA level in unstimulated NR8383 cells. In 10 ng/mL LPS-stimulated cells, IL-10 and IFN- γ reduced CRLR mRNA level at 6 hours from 12.2-fold basal level to 8.0-fold and 5.6-fold, respectively ($P < 0.05$), whereas IL-6 increased the CRLR mRNA level to 16.9-fold ($P < 0.05$). LPS reduced RAMP-2 expression to 0.35-fold basal level at 6 and 12 hours.

AMBP-1 expression was not altered by LPS, but IFN- γ significantly reduced AMBP-1 mRNA level in unstimulated and LPS-stimulated cells to 0.66-fold and 0.47-fold of basal level, respectively, at 6 hours (Fig 1).

IFN- γ at 10 ng/mL increased AM concentration in the culture medium from 12.9 ± 2.3 fmol/mL to 215.9 ± 35.7 fmol/mL ($P < 0.05$), whereas addition of IFN- γ to LPS-stimulated cells increased AM concentration from 120.6 ± 23.8 fmol/mL to 329.7 ± 58.4 fmol/mL ($P < 0.05$).

Effect of AM and AMBP-1 on inflammatory cytokine production in NR8383 and PMA-activated THP-1 cells

AMBP-1 at 500 nM did not alter the concentration of TNF- α , IL-6, or IL-10 in LP-stimulated macrophages. IL-10 secretion from unstimulated NR8383 cells was undetectable and not increased by AM. LPS stimulated IL-10 production that was augmented by 100 nM AM (Fig 2a).

PCR products of IL-10 and TBP are shown (Fig 2b). IL-10 mRNA expression was significantly up-regulated at 6 hours after LPS, paralleled the IL-10 peptide levels and further increased by 140%, 120%, and 65%, with addition of exogenous AM for LPS at 1, 5, and 100 ng/mL, respectively (Fig 2c). LPS-induced IL-10 production was also increased by TNF- α and IL-6 by 71% and 70%, respectively, but was markedly reduced by IFN- γ by 82% (Fig 2d).

In PMA-activated THP-1 cells, LPS markedly increased IL-10 production from as low as 1 ng/mL. 100 nM AM increased LPS-induced IL-10 production by 69% to 112% while IFN- γ reduced it by 77%.

The AM receptor antagonists (AM₂₂₋₅₂ and CGRP₈₋₃₇) did not significantly alter the concentration of TNF- α , IL-6, or IL-10. Pre-incubation with AM followed by washout had no effect on TNF- α , IL-6, or IL-10 production, compared with LPS stimulation alone.

Role of second messenger-dependent kinases in the regulation of AM expression and AM-induced cytokine responses in LPS-stimulated macrophages

Dibutyryl-cAMP (10 μ M) and forskolin (1 μ M) reduced TNF- α production by 50% and increased the production of IL-6 and IL-10 by 105% to 128%. Dibutyryl-cAMP also increased AM concentration from 120.6 \pm 23.8 fmol/mL to 514.5 \pm 102.6 fmol/mL ($P < 0.05$). SQ22536 had no effect on IL-6, IL-10, or AM concentration.

SB203580 inhibited LPS-induced IL-10 production by 56%; the production was partially reversed by exogenous AM and IL-6 but not TNF- α (Fig 3a). In contrast, PD98059 did not significantly affect IL-10 production that could be increased by adding AM or IL-6 (Fig 3b). SB203580 reduced IL-6 production by 13% to 29%; the production was completely reversed by adding AM or TNF- α (Fig 3c). PD98059 reduced IL-6 production by 22% to 26%; the production was reversed by AM but not TNF- α (Fig 3d).

In PMA-activated human THP-1 cells, PD98059 had no effect on LPS-induced IL-10 production but SB203580 inhibited it by 66%. This blockade was not reversible by AM, TNF- α , or IL-6.

PKA-inhibitor did not significantly affect IL-6 and IL-10 production. PKC-inhibitor reduced IL-6 production by 32% ($P < 0.05$), but did not alter IL-10 production. Genistein reduced both IL-6 and IL-10 production by 87%. IL-6 production was partially restored by exogenous AM, but IL-10 production was not rescued by AM, TNF- α , or IL-6.

Discussion

In this study, LPS increased the initial expression of CRLR but reduced the expression of RAMP-2. Expression of CRLR in LPS-stimulated cells was attenuated by IL-10. This might suggest a negative feedback or dampening effect of IL-10 on CRLR expression. IFN- γ increased AM production in LPS-stimulated cells, while it reduced both CRLR and AMBP-1 expression.

In this study, AM significantly augmented LPS-induced IL-10 production in both NR8383 alveolar

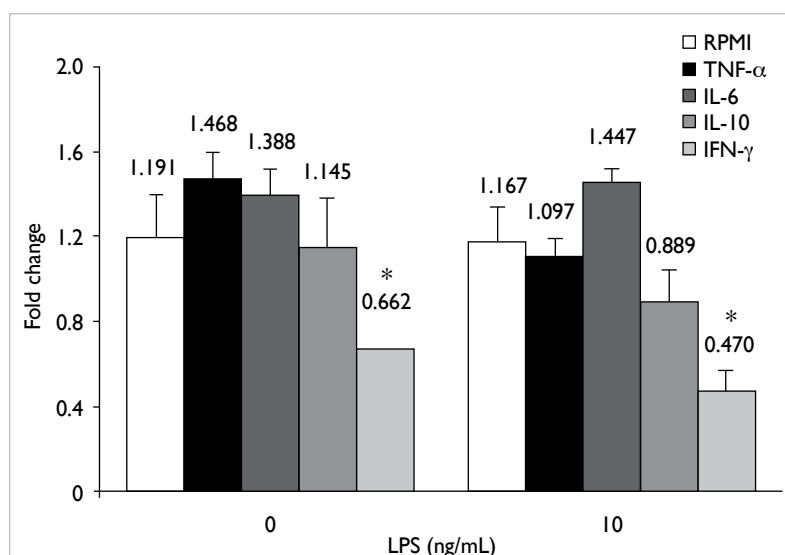


FIG 1. Relative expression of adrenomedullin-binding protein-1 (AMBP-1) in NR8383 cells in response to lipopolysaccharide (LPS) and inflammatory mediators at 6 hours

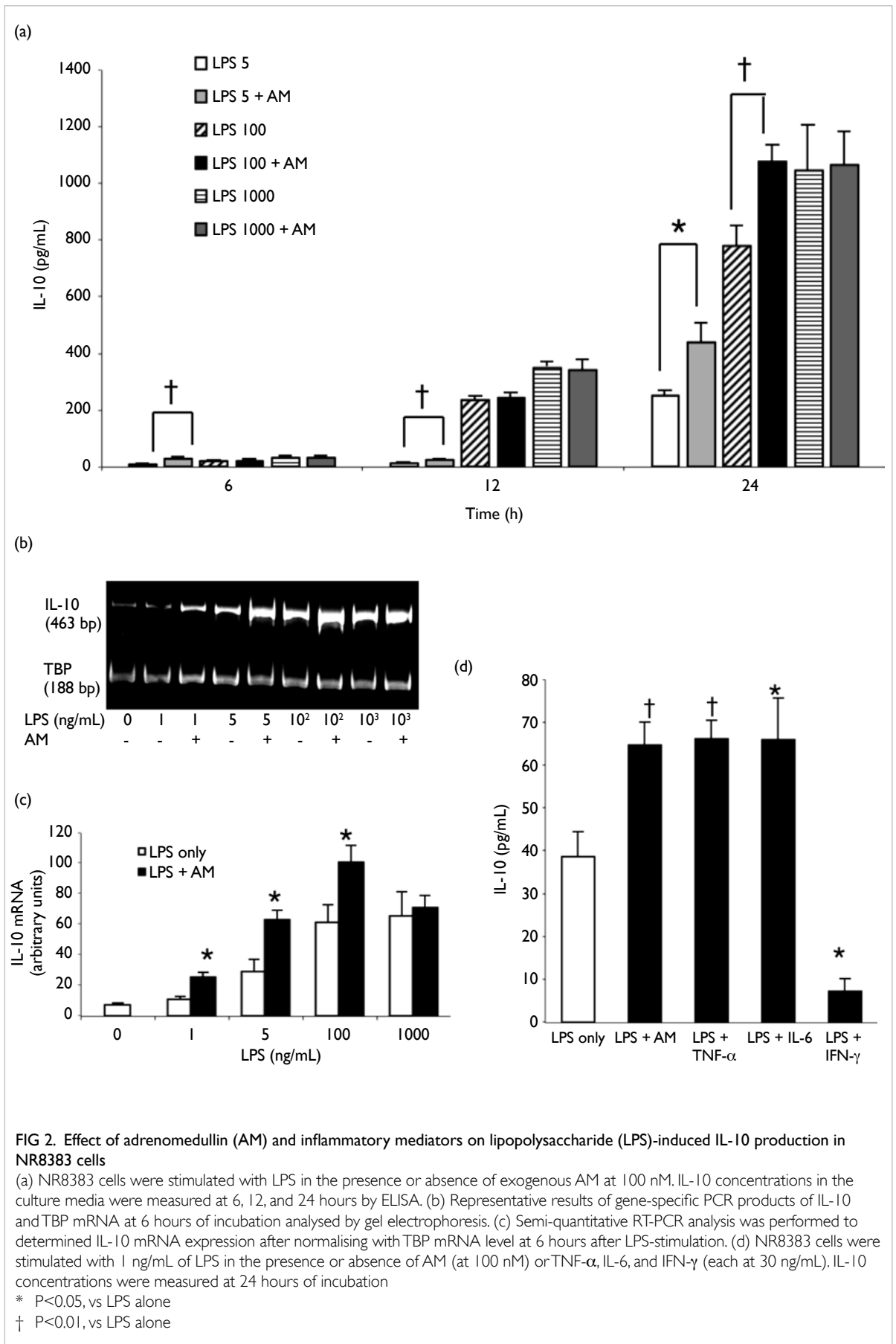
NR8383 cells were stimulated by different inflammatory mediators in the presence or absence of LPS. Expressions of AMBP-1 mRNA were measured by real-time PCR at 6 hours of incubation

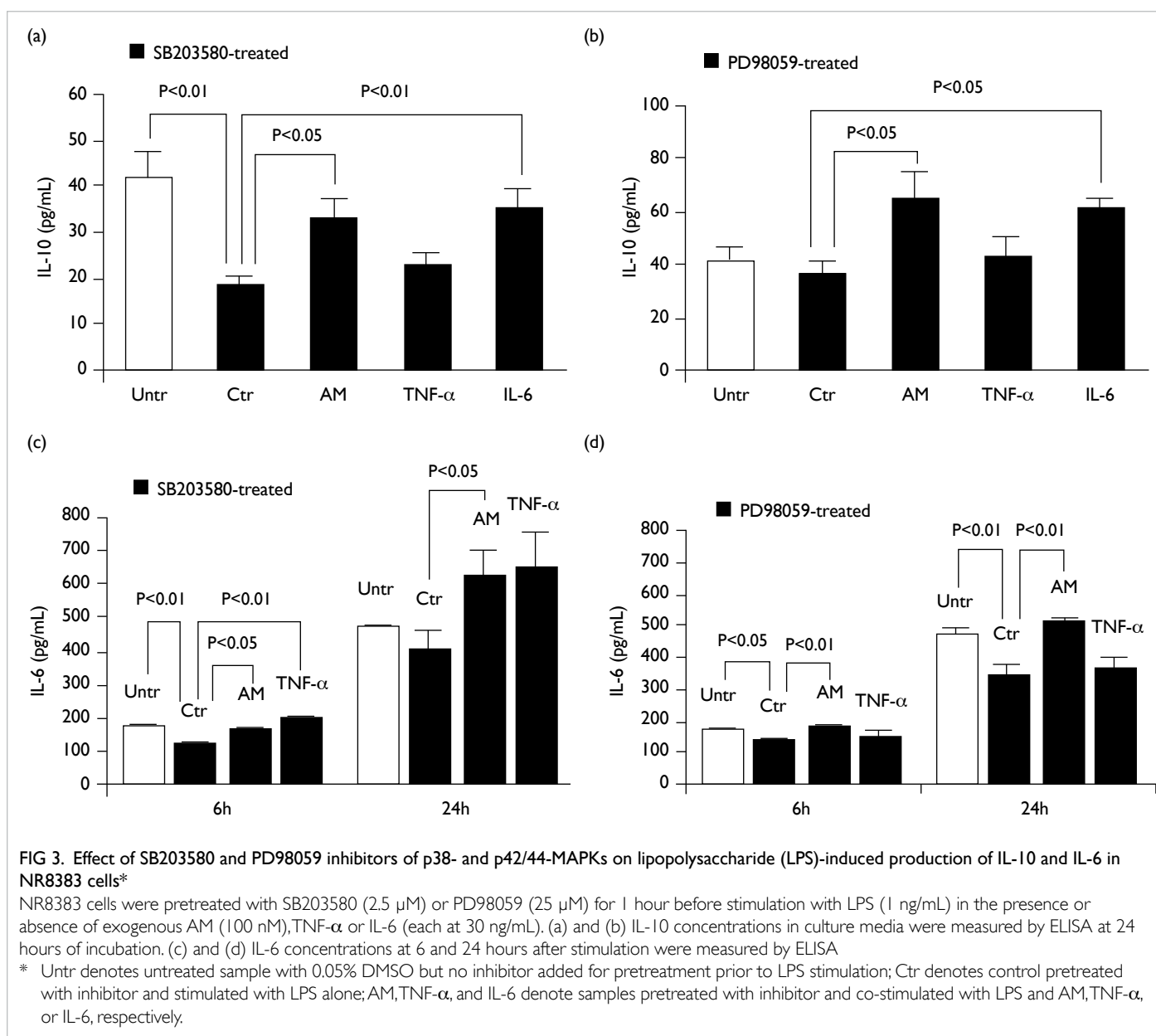
* $P < 0.05$, vs no inflammatory mediator

macrophages and PMA-activated THP-1 cells. This indicates a role of AM production in macrophages and 'macrophage-like' cells. On the contrary, AM receptor antagonists had no significant effect on the production of these inflammatory cytokines on LPS-stimulated NR8383 cells. These indicate that other mediators or alternative pathways independent of AM may be sufficient to stimulate the IL-10 production in these cells. Furthermore, IFN- γ reduced LPS-induced IL-10 production in both NR8383 alveolar macrophages and PMA-activated THP-1 cells that might be related to its inhibitory effect on the AM receptor and AMBP-1 expression. Thus, AM and IFN- γ might have opposite roles in the regulation of the anti-inflammatory cytokine IL-10 in both rat and human macrophages.

In this study, cAMP mediated the increased expression of AM, IL-6 and IL-10, and the decreased expression of TNF- α following LPS stimulation. Moreover, the production of IL-6 was mediated by p38-MAPK, p42/44-MAPK, PKC, and PTK, whereas that of IL-10 was mediated by p38-MAPK and PTK. Activation of the p42/44- and p38-MAPK pathways is common early signals necessary for LPS-induced cytokine production in monocytes and macrophages.⁷

In this study, blockade of the p38-MAPK pathway by SB203580 could be reversed by exogenous AM and IL-6, suggesting that other





pathways may exist to induce IL-10 production upon LPS-stimulation. LPS-induced IL-10 and IL-6 production were markedly reduced by genistein, indicating that PTK-mediated pathways play an important role. The fact that IL-10 synthesis could not be rescued by any of the mediators that increase IL-10 production indicates a decisive role of PTKs in IL-10 production in this macrophage cell line. In contrast, IL-6 production could be partially rescued by AM in the presence of genistein, suggesting that AM activates more than one pathway to induce IL-6 production.

Conclusions

IFN- γ increases the expression of AM but

downregulates CRLR and AMBP-1. AM augments LPS-induced IL-10, independently of increases in TNF- α and IL-6, and acts in opposition to IFN- γ . cAMP mediates the increased expression of AM, IL-6, and IL-10, and the decreased expression of TNF- α following LPS stimulation. The production of IL-6 is mediated by p38-MAPK, p42/44-MAPK, PKC and PTK, whereas that of IL-10 is mediated by p38-MAPK and PTK. AM plays a role in the regulation of inflammation. It augments the production of IL-10, a cytokine that limits inflammation. Nonetheless, the effectiveness of AM, although elevated in inflammation, may be diminished by IFN- γ that down-regulates AM's receptor and its binding protein. The downstream pathways that

mediate IL-10 and IL-6 production are identified. These findings suggest new targets for therapeutic intervention.

Acknowledgements

This study was supported by the Research Fund for the Control of Infectious Diseases, Food and Health Bureau, Hong Kong SAR Government (#05050082). Vivian Chan and Garry Chang contributed to the project as research assistants.

References

1. Cheung BM, Li CY, Wong LY. Adrenomedullin: its role in the cardiovascular system. *Semin Vasc Med* 2004;4:129-34.
2. Wong LY, Cheung BM, Li YY, Tang F. Adrenomedullin is both proinflammatory and antiinflammatory: its effects on gene expression and secretion of cytokines and macrophage migration inhibitory factor in NR8383 macrophage cell line. *Endocrinology* 2005;146:1321-7.
3. Yang S, Zhou M, Chaudry IH, Wang P. Novel approach to prevent the transition from the hyperdynamic phase to the hypodynamic phase of sepsis: role of adrenomedullin and adrenomedullin binding protein-1. *Ann Surg* 2002;236:625-33.
4. Pio R, Martinez A, Unsworth EJ, et al. Complement factor H is a serum-binding protein for adrenomedullin, and the resulting complex modulates the bioactivities of both partners. *J Biol Chem* 2001;276:12292-300.
5. Yang S, Zhou M, Fowler DE, Wang P. Mechanisms of the beneficial effect of adrenomedullin and adrenomedullin-binding protein-1 in sepsis: down-regulation of proinflammatory cytokines. *Crit Care Med* 2002;30:2729-35.
6. Li YY, Cheung BM, Hwang IS, Wong LY, Kumana CR, Tang F. Adrenomedullin gene expression and levels in the cardiovascular system after treatment with lipopolysaccharide. *Neuropeptides* 2005;39:73-80.
7. Foey AD, Parry SL, Williams LM, Feldmann M, Foxwell BM, Brennan FM. Regulation of monocyte IL-10 synthesis by endogenous IL-1 and TNF-alpha: role of the p38 and p42/44 mitogen-activated protein kinases. *J Immunol* 1998;160:920-8.

Association of human adenovirus-36 with diabetes, adiposity, and dyslipidaemia in Hong Kong Chinese

MMY Waye *, JCN Chan, PCY Tong, R Ma, PKS Chan

KEY MESSAGES

1. Adenovirus-36 (Ad-36) is the only human adenovirus currently known to be associated with human obesity.
2. The Ad-36 antibody and Ad-36 DNA in both the plasma and stool of four groups of subjects stratified by diabetes and obesity status were examined.
3. Although the detection rate of Ad-36 plasma DNA was similar among the four groups, participants with obesity or diabetes had a higher rate of Ad-36 infection. In addition, participants with Ad-36 infection had lower high-density lipoprotein (HDL) than those without.

Nonetheless, the lower HDL in Ad-36 positive subjects may be confounded by age, obesity and diabetes status.

Hong Kong Med J 2015;21(Suppl 4):S45-7

RFCID project number: 08070082

¹ MMY Waye *, ² JCN Chan, ² PCY Tong, ³ R Ma, ⁴ PKS Chan

¹ School of Biomedical Sciences, The Chinese University of Hong Kong

² Department of Medicine and Therapeutics, The Chinese University of Hong Kong

³ Department of Medicine, Prince of Wales Hospital

⁴ Department of Microbiology, The Chinese University of Hong Kong

* Principal applicant and corresponding author: mary-waye@cuhk.edu.hk

Introduction

Obesity is a major health concern.¹ The first report of obesity caused by a virus was published in 1982,² and four other animal viruses have been identified since. Of the 51 human adenoviruses, three have been shown to cause obesity in animal models, whereas two have not.^{3,4} This study aimed to examine the association of human adenovirus-36 (Ad-36) with diabetes, adiposity, and dyslipidaemia in Hong Kong Chinese.

Methods

Ethical approval was obtained from the CUHK Clinical Research Ethics Committee. The body mass index (BMI) cut-off value was defined as 23 kg/m² for overweight and 25 kg/m² for obesity. This study was conducted from April 2009 to March 2011. A total of 303 serum samples were collected from four groups of local Chinese subjects aged 25 to 55 years with no family history of diabetes: (1) non-obese (BMI <23 kg/m²) non-diabetic controls (n=72), (2) obese (BMI ≥25 kg/m²) non-diabetic subjects (n=93), (3) obese diabetic subjects (n=70), and (4) non-obese diabetic subjects (n=68).

Results

Adenovirus-36 DNA in serum samples

A pair of primers was designed to study Ad-36. The specificity of the primers was evaluated with

adenoviruses serotype 1 to 6. A few unspecific bands in the other serotypes were observed with the naked eye, but they were very low in intensity and did not significantly affect the analyses (Fig). All 303 serum samples were screened with PCR assay using set B primer.

The Ad-36 DNA band size 149bp was amplified with set B primer. Among the 4 groups, non-obese diabetic subjects had the highest positive rate, followed by obese non-diabetic subjects, obese diabetic subjects, and non-obese non-diabetic subjects. The positive rate for the obese and non-obese groups was 7.4% and 7.1%, respectively (P=0.5608, Table 1).

Isolation of Ad-36 DNA from serum was technically challenging. Although positive controls using Ad-36 DNA as a template gave a DNA sequence that matched 100% with the expected published sequence, direct sequencing of the PCR from serum samples did not generate good sequence information, probably owing to an extremely low yield of PCR products. PCR with the primer set C yielded no bands with the serum DNA samples.

Antibody neutralisation tests

Antibodies in the sera were assayed by antibody neutralisation tests using Ad-36 grown in A549 cells. Each test serum was run in duplicate with a serum control (serum and cells, no virus), cell control (cells only, no serum, no virus) and virus control (cells and virus, no serum). Serum samples were considered

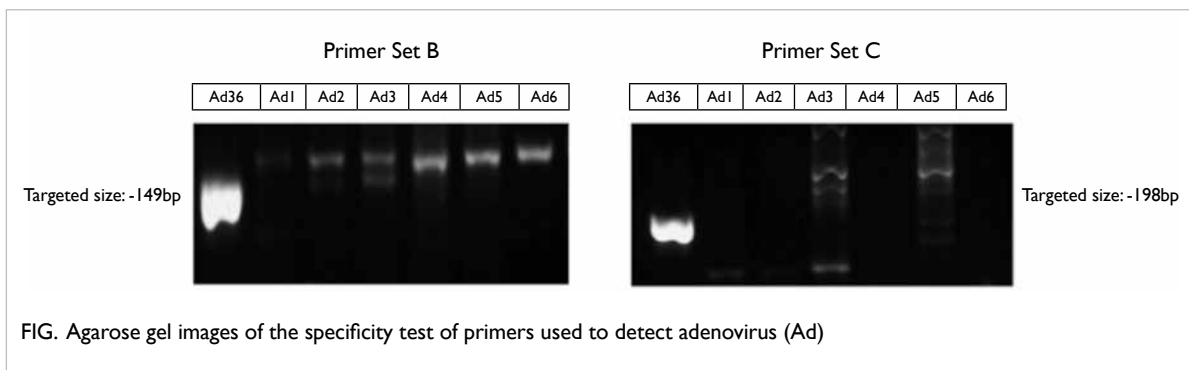


FIG. Agarose gel images of the specificity test of primers used to detect adenovirus (Ad)

TABLE 1. Adenovirus-36 DNA positive rates for the four groups stratified by diabetes and obesity status and the overall obese and non-obese groups

Group	No. (%) of subjects			
	Strong band	Weak band	No band	Positive rate
Non-obese non-diabetic (controls, n=72)	1 (1.39)	2 (2.78)	69 (95.83)	3 (4.1)
Obese non-diabetic (n=93)	3 (3.23)	5 (5.38)	85 (91.40)	8 (8.6)
Obese diabetic (n=70)	2 (2.86)	2 (2.86)	66 (94.29)	4 (5.7)
Non-obese diabetic (n=68)	2 (2.94)	5 (7.35)	61 (89.71)	7 (10.3)
Overall*				
Obese (n=163)	5 (6.09)	7 (8.24)	151 (92.6)	12 (7.4)
Non-obese (n=140)	3 (4.33)	7 (10.13)	130 (92.9)	10 (7.1)

* P=0.5608, Fisher's exact test one-tailed probability

TABLE 2. Antibody neutralisation test for adenovirus-36

Variable	Total (n=174)	Ad-36 positive (n=30)	Ad-36 negative (n=144)	P value (t test or Chi squared test)
Mean±SD age (years)	45.9±7.3	49.6±4.4	45.2±7.5	0.002
No. (%) of females	95 (54.6)	17 (56.7)	78 (54.2)	0.843
No. (%) of obesity	80 (46.0)	18 (60.0)	62 (43.1)	0.090
No. (%) of diabetes	132 (75.9)	28 (93.3)	104 (72.2)	0.014

TABLE 3. Stool DNA PCR results

Group	No. (%) of adenovirus-36 DNA in stool	P value
Obese (n=100)	11 (11)	0.34
Non-obese (n=67)	11 (16)	
Diabetic (n=63)	12 (19)	0.132
Non-diabetic (n=104)	12 (12)	
Non-obese non-diabetic (n=53)	6 (11)	0.132
Non-obese diabetic (n=14)	5 (35)	
Obese non-diabetic (n=51)	4 (7)	0.24
Obese diabetic (n=49)	7 (14)	

to contain neutralising antibodies when 50% of the wells showed a cytopathic effect. Obese subjects had a higher percentage of antibody-positive samples than non-obese subjects (Table 2).

Stool DNA analyses

Stool DNA was also studied by PCR using primer set B. The positivity rate of Ad-36 DNA in the stool was higher in non-obese diabetic subjects than non-obese non-diabetic subjects (35% vs 11%, P=0.042). Stool samples were insufficient to use the nanodrop PCR method to amplify the DNA, thus many stool samples had an undetectable level of DNA. The results of the Ad-36 DNA study in stool samples using primer set B are shown in Table 3.

Discussion

Of 278 participants, 174 had valid measures of lipid profile. Participants with Ad-36 infection were older and more likely to have diabetes, compared with participants without Ad-36 infection. In addition, there was a marginal difference in obesity between participants with and without Ad-36 infection. Participants with Ad-36 infection had significantly

lower high-density lipoprotein (HDL) than those without (1.30 ± 0.37 mmol/L vs 1.49 ± 0.44 mmol/L), although this difference was not significant after adjusting for confounding factors (age, sex, obesity, and diabetes). No significant difference was noted in total cholesterol, triglycerides, or low-density lipoprotein in either univariate analyses or multivariate analyses (data not shown).

The rate of Ad-36 DNA in stool samples (antibody positive rate) was higher in non-obese diabetic subjects than non-obese non-diabetic subjects (35% vs 11%, $P=0.042$). Two possible reasons for the slightly higher rate in our group compared with other studies are: (1) the cut-off point to define our obese subjects was lower, as we applied the Asian definition of obesity rather than that of the World Health Organization. Thus, the categorisation of BMI in obesity classes based on co-morbidity risk might not operate for adiposity related to adenovirus infection. (2) Microbes other than Ad-36 virus might be more relevant in Hong Kong with regard to their role in the pathogenesis of obesity. In support of this notion, we incidentally detected a higher rate of a 200 bp band in the obese group, compared with the non-obese group. Upon cloning and sequence analyses, it is suggested that another microbe might be associated with obesity. The identity of the microbe is not certain but our preliminary results indicate that its DNA sequence matches that of *Babesia gibsoni* 16S ribosomal RNA (data not shown).

Conclusions

Obese or diabetic subjects had a higher rate of Ad-36

infection. Those with Ad-36 infection also had lower HDL than those without, but this finding may have been confounded by age, obesity and diabetes status. Non-obese diabetic subjects had a higher rate of Ad-36 DNA in the stool than non-obese non-diabetic subjects. These findings support the possible role of viral or microbial infection in both obesity and diabetes, although larger cohort studies together with mechanistic studies are needed to confirm these findings.

Acknowledgements

This study was supported by the Research Fund for the Control of Infectious Diseases, Food and Health Bureau, Hong Kong SAR Government (#08070082). The authors thank all subjects for their participation and all assistants and students for their assistance.

References

1. Wang Y, Beydoun MA, Liang L. <http://www.nature.com/oby/journal/v16/n10/abs/oby2008351a.html>.
2. Wang Y, Beydoun MA, Liang L, Caballero B, Kumanyika SK. Will all Americans become overweight or obese? Estimating the progression and cost of the US obesity epidemic. *Obesity (Silver Spring)* 2008;16:2323-30.
2. Lyons MJ, Faust IM, Hemmes RB, Buskirk DR, Hirsch J, Zabriskie JB. A virally induced obesity syndrome in mice. *Science* 1982;216:82-5.
3. Dhurandhar NV, Israel BA, Kolesar JM, Mayhew GF, Cook ME, Atkinson RL. Increased adiposity in animals due to a human virus. *Int J Obes Relat Metab Disord* 2000;24:989-96.
4. Dhurandhar NV, Whigham LD, Abbott Dh, et al. Human adenovirus Ad-36 promotes weight gain in male rhesus and marmoset monkeys. *J Nutr* 2002;132:3155-60.

AUTHOR INDEX

Chan HLY	22, 31	Luan J	31
Chan JCN	45	Ma R	45
Chan KS	4	Mok TYW	4
Chan PKS	45	Ng IOL	27
Chan WM	20	Ng S	20
Chen HL	12	Poon TCW	22
Cheung BMV	39	Sung JYJ	22, 31
Cheung CY	8	Sze KMF	27
Cho CH	17	Tam CM	4
Chu GKY	27	Tian LW	20
Ding CM	31	Tong PCY	45
Fung J	35	Waye MMY	45
Guan Y	12	Wong DKH	35
Ho PL	4	Wong LYF	39
Ho SC	20	Wong WY	20
Huang JD	14	Wu WKK	17
Hui AY	22	Yam WC	4
Lai CL	35	Yew WW	4
Lau RHY	22	Yu J	17
Lee MY	8	Yuen KY	14
Leung CC	4	Yuen MF	35
Leung HWC	22	Zhang L	17
Lo A	22	Zheng BJ	14
Lok S	8		

Disclaimer

The reports contained in this publication are for reference only and should not be regarded as a substitute for professional advice. The Government shall not be liable for any loss or damage, howsoever caused, arising from any information contained in these reports. The Government shall not be liable for any inaccuracies, incompleteness, omissions, mistakes or errors in these reports, or for any loss or damage arising from information presented herein. The opinions, findings, conclusions and recommendations expressed in this report are those of the authors of these reports, and do not necessarily reflect the views of the Government. Nothing herein shall affect the copyright and other intellectual property rights in the information and material contained in these reports. All intellectual property rights and any other rights, if any, in relation to the contents of these reports are hereby reserved. The material herein may be reproduced for personal use but may not be reproduced or distributed for commercial purposes or any other exploitation without the prior written consent of the Government. Nothing contained in these reports shall constitute any of the authors of these reports an employer, employee, servant, agent or partner of the Government.

Published by the Hong Kong Academy of Medicine Press for the Government of the Hong Kong Special Administrative Region. The opinions expressed in the *Hong Kong Medical Journal* and its supplements are those of the authors and do not reflect the official policies of the Hong Kong Academy of Medicine, the Hong Kong Medical Association, the institutions to which the authors are affiliated, or those of the publisher.